
The Radiation and Scattering of Surface Waves by a Vertical Circular Cylinder in a Channel

C. M. Linton and D. V. Evans

Phil. Trans. R. Soc. Lond. A 1992 **338**, 325-357

doi: 10.1098/rsta.1992.0011

Email alerting service

Receive free email alerts when new articles cite this article - sign up in the box at the top right-hand corner of the article or click [here](#)

To subscribe to *Phil. Trans. R. Soc. Lond. A* go to:
<http://rsta.royalsocietypublishing.org/subscriptions>

The radiation and scattering of surface waves by a vertical circular cylinder in a channel

BY C. M. LINTON AND D. V. EVANS

University of Bristol, University Walk, Bristol BS8 1TW, U.K.

Contents

	PAGE
1. Introduction	325
2. Channel multipoles	328
3. The general radiation problem	335
4. The scattering problem	341
5. Truncated cylinders	345
6. Conclusion	355
Appendix. Behaviour of channel multipoles near cut-off frequencies	356
References	356

In this paper we consider the problems of the radiation and scattering of surface gravity waves by a vertical circular cylinder placed on the centreline of a channel of width $2d$ and depth H , and either extending from the bottom through the free surface or truncated so as to fill only part of the depth. These problems are solved, for arbitrary incident wavenumber k , by constructing appropriate multipoles for cylinders placed symmetrically in channels and then using the body boundary condition to derive a set of infinite systems of linear algebraic equations. For the general problems considered here, this method is superior to the more usual approach of using a set of image cylinders to model the channel walls, in particular the occurrence of modes other than the fundamental when $kd > \frac{1}{2}\pi$ is accurately modelled and the correct form predicted for the far-field.

1. Introduction

In three recent papers (Çalişal & Sabuncu 1989; Yeung & Sphaier 1989*a, b*, hereafter referred to as I, II and III respectively) problems concerning the hydrodynamic properties of a vertical circular cylinder, immersed through the free surface and extending part way to the bottom, situated in the centre of a channel have been considered using linear water wave theory. One reason for interest in these problems is because of the need to know how the side walls of a wave tank affect the results of experiments on relatively large models. Many of the problems associated with the solution of such problems can be explained with reference to much simpler problems and so we will begin by considering one such problem here.

We will examine the problem of a plane wave incident on a vertical circular cylinder that extends throughout the fluid depth and is placed symmetrically in a wave tank. Owing to the constant depth variation in this problem and the symmetry

Phil. Trans. R. Soc. Lond. A (1992) **338**, 325–357

Printed in Great Britain

325

of the geometry, the problem is equivalent to the two-dimensional acoustic scattering of a wave normally incident upon an infinite array of equally-spaced identical circular cylinders, a problem with a very long history (see, for example, von Ignatowsky 1914, 1915; Lamb 1945, p. 537). There are many methods of solution for this problem including the multiple scattering method of Twersky (1952) and the use of Green's functions (Twersky 1956, 1962) but the most often used is an extension of a direct method of solution devised by Závřiska (1913) for the scattering of an incident plane wave by a finite array of circular cylinders. In the context of water waves these methods were first used by Spring & Monkmeyer (1974) for the finite array case and by Spring & Monkmeyer (1975) for the case of an infinite row of cylinders, whereas Linton & Evans (1990) provided a major simplification to the solution for the case of a general array. The problem of the radiation and scattering of surface waves by an infinite row of submerged ducts was considered, using essentially an extension of the method of Twersky (1962), by Miles (1983) from the point of view of wave energy absorption.

The main idea of the direct method is to express the total velocity potential as a sum of an incident wave and a general circular wave emanating from each cylinder in the array. In the case of a plane wave normally incident on an infinite row of identical cylinders all these circular waves will be identical and thus the body boundary condition need only be applied on one cylinder. By using Graf's addition theorem for Bessel functions these circular waves can be expressed in terms of coordinates centred on one particular cylinder and then the boundary condition can be applied on that cylinder giving rise to an infinite system of linear algebraic equations. To solve such a system numerically a truncation procedure must be used and this corresponds to using only a finite number of circumferential modes to represent the cylindrical waves. This method forms the basis of the solution procedure used in II and III.

In I a slightly different, and less satisfactory, procedure is used. They consider the case of a cylinder situated in the middle of a row of N cylinders (in fact they use $N = 3$) and use this as an approximation to an infinite row of cylinders. This approach has a major drawback due to the fact that the solution to the problem with an infinite row of cylinders is inherently two-dimensional, whereas any problem concerned with a finite array of cylinders is not. It is well known that at any given wavenumber a finite number of propagating modes can exist in a channel and that as the wavenumber increases so does the number of modes. In fact if k is the wavenumber and the channel width is $2d$ then if $(j-1)\pi < kd < (j-\frac{1}{2})\pi$, ($j \geq 1$) j modes are possible. Thus if an incident wave is scattered by a cylinder in a channel there will be up to j reflected and j transmitted propagating modes. The far field at $x = \pm \infty$ will therefore look like a finite sum of plane waves. However, if we model the situation by a row of N cylinders then however large we take N , sufficiently far away from the cylinder group the wave field will look like an outgoing circular wave and so the far-field behaviour can never be accurately modelled.

In theory the method used by Spring & Monkmeyer (1975) which forms the basis for the analysis used in II and III does not suffer from this drawback since all the 'image' cylinders are taken into account. However in this formulation the velocity potential is described in terms of an infinite sum of circular waves, each centred at a different point, each one of which is only known approximately from the solution to a truncated system of equations and so predicting the correct far-field behaviour is still virtually impossible.

Another difficulty which arises when using this method is the occurrence of slowly-convergent Hankel series as is described in Thomas (1991) though a careful treatment involving integral representations can alleviate the problems, as was done in II and III. Finally the method becomes fairly unwieldy when used to solve problems involving truncated cylinders and in II and III the authors found it necessary to neglect the (albeit small) interference effects caused by non-propagating modes.

In this paper we will consider problems involving circular cylinders in channels using a fundamentally different method which correctly predicts the far-field behaviour, avoids the treatment of slowly convergent series and is, in principle, exact. The method is based around the construction of suitable multipoles for channel problems. Thus when considering a channel of water of depth H and width $2d$ suitable multipoles will be solutions of Laplace's equation in $-\infty < x < \infty$, $|y| \leq d$, $-H \leq z \leq 0$ which are singular at $(x, y) = (0, 0)$ and which satisfy the condition of zero normal velocity on $|y| = d$. They must also look like outgoing plane waves as $|x| \rightarrow \infty$ or else be exponentially small there. The key to the construction of these multipoles is the derivation of suitable integral representations for solutions to Laplace's equation in a laterally unbounded fluid which can then be modified to take account of the channel walls using a technique similar to that used by Thorne (1953). The procedure is fairly complicated but picks out the correct far-field behaviour in a natural way.

Once the multipoles have been constructed a wide class of problems can be solved in a straightforward manner including both scattering and radiation problems, problems involving cylinders which occupy the whole depth of fluid and problems involving truncated cylinders, either occupying $-H \leq z \leq -D$ or $-D \leq z \leq 0$, ($D < H$).

In a recent paper Callan *et al.* (1991) proved the existence of trapped modes in the presence of a circular cylinder extending throughout the water depth placed symmetrically in a channel. In this paper it was proved that for a cylinder of any radius $a < d$ a trapped mode which is antisymmetric about $y = 0$ exists at some value of kd less than the first antisymmetric cut-off frequency $\frac{1}{2}\pi$. In this problem trapped modes are solutions to the homogeneous boundary-value problem (zero normal derivative on all solid boundaries) where no waves are radiated down the channel and thus represent modes of finite energy. Clearly the presence of a solution to the homogeneous problem implies the non-uniqueness of the solution to a forcing problem at that frequency and so we expect singular behaviour in the solutions to problems which are antisymmetric about the centreline of the channel at certain discrete frequencies.

In §2 channel multipoles are constructed and expansions in polar coordinates developed. A general radiation problem for the vertical cylinder extending throughout the depth is considered in §3 in which a general condition on the normal fluid velocity on the cylinder is imposed. The problem is reduced to the solution of sets of infinite systems of equations where the right-hand sides involve the Fourier coefficients of the general boundary condition on the cylinder. Attention is then given to surge and sway motion of a rigid cylinder and in particular to the computation of the added mass and damping coefficients. A global relation between the damping coefficient and the far-field amplitude is used as a check on the results.

In §4 the scattering by the cylinder of an incident plane wave is considered and shown to be a particularly simple example of the general formulation given in §3. The

number of multipoles required to achieve accurate results in this case is extremely small. In addition to computation of the reflection and transmission coefficients for the different modes, computations are also made of the first-order oscillatory force and the mean second-order force on the cylinder.

Both the scattering problem and the radiation problems of surge, sway and heave for truncated cylinders are considered in §5 where now appropriate eigenfunctions for an interior fluid region are needed to match with the multipole potentials across the common fluid boundary. The resulting sets of infinite systems of equations are no longer uncoupled as was the case for the cylinder extending throughout the depth where a separate infinite system was obtained for each depth mode. Curves are presented of the added mass and damping coefficients in all modes of oscillation as well as the fundamental reflection coefficient for the scattering problem for this case.

The values of kd for which trapped modes occur are also determined, which confirm and extend the results of Callan *et al.* (1991).

2. Channel multipoles

Cartesian axes are chosen with the mean free surface the xy plane and z measured vertically upwards, the fluid bottom being $z = -H$. The fluid is contained in a channel, the sides of which are $|y| = d$, $-\infty < x < \infty$. We will derive expressions for multipoles suitable for the solution of Laplace's equation in such a channel. With the usual assumptions of an inviscid, incompressible fluid there exists a harmonic velocity potential $\Phi(x, y, z, t)$. It is further assumed that all motion is time-harmonic with angular frequency ω and so assuming the linear theory of irrotational surface waves we can write

$$\Phi(x, y, z, t) = \Re\{\phi(x, y, z) e^{-i\omega t}\}. \quad (2.1)$$

The condition that must be satisfied on the mean free surface ($z = 0$) is

$$K\phi = \partial\phi/\partial z, \quad (2.2)$$

where $K = \omega^2/g$. Separation of variables shows that suitable depth eigenfunctions for this problem are

$$f_m(z) = M_m^{-\frac{1}{2}} \cos k_m(z + H), \quad (2.3)$$

where

$$M_m = \frac{1}{2}(1 + \sin 2k_m H / 2k_m H) \quad (2.4)$$

and k_m satisfies

$$k_m \tan k_m H + K = 0. \quad (2.5)$$

Here $k_m, m \geq 1$, are real and positive, while $k_0 = ik$, k real and positive. The functions $f_m(z)$ satisfy the orthogonality relations

$$\frac{1}{H} \int_{-H}^0 f_m(z) f_n(z) dz = \delta_{mn}. \quad (2.6)$$

Specifically then we look for functions $\phi_{n,m}^s(x, y)$, symmetric about the centreline of the channel, and $\phi_{n,m}^a(x, y)$, antisymmetric about this line, which satisfy

$$(\nabla^2 - k_m^2) \phi_{n,m}^s = (\nabla^2 - k_m^2) \phi_{n,m}^a = 0 \quad 0 < y < d, \quad n, m = 0, 1, \dots, \quad (2.7)$$

$$\partial\phi_{n,m}^s/\partial y = \partial\phi_{n,m}^a/\partial y = 0 \quad \text{on } y = d, \quad (2.8)$$

$$\partial\phi_{n,m}^s/\partial y = 0 \quad \text{on } y = 0, \quad (2.9)$$

and
$$\phi_{n,m}^a = 0 \quad \text{on } y = 0. \quad (2.10)$$

These functions will be singular at the origin and will decay exponentially as $|x| \rightarrow \infty$ if $m \geq 1$, whereas if $m = 0$ they will behave like outgoing plane waves as $|x| \rightarrow \infty$. Polar coordinates defined by

$$x = r \cos \theta, \quad y = r \sin \theta,$$

will also be used.

In the absence of the channel walls appropriate choices for $\phi_{n,m}^s$ are $H_n^{(1)}(kr) \cos n\theta$ for $m = 0$ and $K_n(k_m r) \cos n\theta$ for $m \geq 1$, which are even about $\theta = \frac{1}{2}\pi$ ($x = 0$) if n is even and odd about this line if n is odd. For $\phi_{n,m}^a$ we replace $\cos n\theta$ by $\sin n\theta$ in these formulas. It should be pointed out that we could equally well use $H_n^{(2)}$ in the following procedure, the resulting multipoles would be the same. There are many possible integral representations that can be used as starting points in the construction of channel multipoles. Here we choose

$$H_n(kr) = -\frac{1}{\pi} \int_{a+i\infty}^{b-i\infty} e^{ikr \cos \omega} e^{in(\omega-\pi/2)} d\omega, \quad -\pi < a < 0, \quad 0 < b < \pi, \quad (2.11)$$

(Erdélyi *et al.* 1953, p. 20), where for simplicity we have written H_n for $H_n^{(1)}$, and

$$K_n(k_m r) = \frac{1}{2}i \int_{a+i\infty}^{b-i\infty} e^{-k_m r \cos \omega} e^{in\omega} d\omega, \quad -\frac{1}{2}\pi < a, b < \frac{1}{2}\pi, \quad (2.12)$$

(Erdélyi *et al.* 1953, p. 24). The Hankel function case will now be considered in detail. A simple change of variable leads to

$$H_n(kr) i^n e^{in\theta} = -\frac{i}{\pi} \int_{i(a+\theta)-\infty}^{i(b+\theta)+\infty} e^{ikx \cosh \alpha} e^{ky \sinh \alpha} e^{n\alpha} d\alpha, \quad -\pi < a < 0, \quad 0 < b < \pi. \quad (2.13)$$

By restricting the range of θ we can make the limits of integration independent of θ . Thus

$$H_n(kr) i^n e^{in\theta} = -\frac{i}{\pi} \int_{-\infty}^{\infty+i\pi} e^{ikx \cosh \alpha} e^{ky \sinh \alpha} e^{n\alpha} d\alpha, \quad 0 < \theta < \pi. \quad (2.14)$$

It follows that

$$H_{2n}(kr) \cos 2n\theta = -(-1)^n \frac{i}{\pi} \int_{-\infty}^{\infty+i\pi} e^{ky \sinh \alpha} \cos(kx \cosh \alpha) e^{-2n\alpha} d\alpha \quad (2.15)$$

and this integral can be converted into a single integral from 0 to ∞ as follows. By splitting the integral into four parts, namely $(-\infty, 0)$, $(0, \frac{1}{2}i\pi)$, $(\frac{1}{2}i\pi, i\pi)$ and $(i\pi, \infty+i\pi)$ and making the substitutions $\alpha = -v$, $\alpha = i(\frac{1}{2}\pi - u)$, $\alpha = i(\frac{1}{2}\pi + u)$ and $\alpha = v + i\pi$ respectively, the following expression is obtained:

$$H_{2n}(kr) \cos 2n\theta = \frac{2}{\pi} \int_0^{\frac{1}{2}\pi} e^{iky \cos u} \cos(kx \sin u) \cos 2nu du \\ - (-1)^n \frac{2i}{\pi} \int_0^\infty e^{-ky \sinh v} \cos(kx \cosh v) \cosh 2nv dv. \quad (2.16)$$

We can also derive

$$H_{2n+1}(kr) \cos(2n+1)\theta = \frac{2}{\pi} \int_0^{\frac{1}{2}\pi} e^{iky \cos u} \sin(kx \sin u) \sin(2n+1)u \, du \\ - (-1)^n \frac{2i}{\pi} \int_0^\infty e^{-ky \sinh v} \sin(kx \cosh v) \cosh(2n+1)v \, dv, \quad (2.17)$$

$$H_{2n+1}(kr) \sin(2n+1)\theta = -\frac{2i}{\pi} \int_0^{\frac{1}{2}\pi} e^{iky \cos u} \cos(kx \sin u) \cos(2n+1)u \, du \\ - (-1)^n \frac{2i}{\pi} \int_0^\infty e^{-ky \sinh v} \cos(kx \cosh v) \sinh(2n+1)v \, dv, \quad (2.18)$$

and

$$H_{2n}(kr) \sin 2n\theta = -\frac{2i}{\pi} \int_0^{\frac{1}{2}\pi} e^{iky \cos u} \sin(kx \sin u) \sin 2nu \, du \\ + (-1)^n \frac{2i}{\pi} \int_0^\infty e^{-ky \sinh v} \sin(kx \cosh v) \sinh 2nv \, dv. \quad (2.19)$$

These integral representations are all valid for $y > 0$.

It is convenient to define the following functions:

$$\gamma(t) = \begin{cases} -i(1-t^2)^{\frac{1}{2}}, & t \leq 1, \\ (t^2-1)^{\frac{1}{2}}, & t > 1, \end{cases} \quad (2.20)$$

$$c_{2n}(t) = \begin{cases} \cos[2n \arcsin t], & t \leq 1, \\ (-1)^n \cosh[2n \operatorname{arcosh} t], & t > 1, \end{cases} \quad (2.21)$$

$$c_{2n+1}(t) = \begin{cases} \cos[(2n+1) \arcsin t], & t \leq 1, \\ i(-1)^n \sinh[(2n+1) \operatorname{arcosh} t], & t > 1, \end{cases} \quad (2.22)$$

$$s_{2n}(t) = \begin{cases} \sin[2 \arcsin t], & t \leq 1, \\ -i(-1)^n \sinh[2n \operatorname{arcosh} t], & t > 1, \end{cases} \quad (2.23)$$

$$s_{2n+1}(t) = \begin{cases} \sin[(2n+1) \arcsin t], & t \leq 1, \\ (-1)^n \cosh[(2n+1) \operatorname{arcosh} t], & t > 1. \end{cases} \quad (2.24)$$

Note that the definitions for $t \leq 1$ and $t > 1$ are equivalent since

$$\operatorname{arcosh} t = i(\arcsin t - \frac{1}{2}\pi).$$

We then make the substitutions

$$u = \arcsin t, \quad v = \operatorname{arcosh} t, \quad (2.25)$$

which leads to

$$H_{2n}(kr) \cos 2n\theta = -\frac{2i}{\pi} \int_0^\infty \gamma^{-1} e^{-k\gamma y} \cos kxt c_{2n}(t) \, dt, \quad (2.26)$$

$$H_{2n+1}(kr) \cos(2n+1)\theta = -\frac{2i}{\pi} \int_0^\infty \gamma^{-1} e^{-k\gamma y} \sin kxt s_{2n+1}(t) \, dt, \quad (2.27)$$

$$H_{2n+1}(kr) \sin(2n+1)\theta = -\frac{2}{\pi} \int_0^\infty \gamma^{-1} e^{-k\gamma y} \cos kxt c_{2n+1}(t) \, dt, \quad (2.28)$$

$$\text{and} \quad H_{2n}(kr) \sin 2n\theta = -\frac{2}{\pi} \int_0^\infty \gamma^{-1} e^{-k\gamma y} \sin kxt s_{2n}(t) dt. \quad (2.29)$$

Multipoles can now be constructed using the method of Thorne (1953). To satisfy the boundary condition on $y = d$ we add to $H_{2n}(kr) \cos 2n\theta$ a function of the form

$$-\frac{2i}{\pi} \int_0^\infty B(t) \cosh k\gamma y \cos kxt c_{2n}(t) dt.$$

Equation (2.8) then implies that

$$B(t) = e^{-k\gamma d} / \gamma \sinh k\gamma d$$

which has singularities for real t . Thus the function

$$\psi_{2n,0}^s = -\frac{2i}{\pi} \int_0^\infty \frac{\cosh [k\gamma(d-y)]}{\gamma \sinh k\gamma d} \cos kxt c_{2n}(t) dt, \quad (2.30)$$

where the integral is taken to be a principal value integral at all the singularities, satisfies both (2.7) with $m = 0$ and (2.8). We need to determine the behaviour of this function as $|x| \rightarrow \infty$.

The integrand, considered as a function of a complex variable t , has simple poles at $k\gamma d = \pm p\pi i$, $p = 0, 1, \dots$, i.e. at $t = \pm t_p$, where

$$t_p = (1 - (p\pi/kd)^2)^{\frac{1}{2}}, \quad p = 0, 1, \dots, j_s, \quad (2.31)$$

$$t_p = i((p\pi/kd)^2 - 1)^{\frac{1}{2}}, \quad p \geq j_s + 1, \quad (2.32)$$

where

$$j_s \pi < kd < (j_s + 1) \pi. \quad (2.33)$$

To determine the behaviour of $\psi_{2n,0}^s$ as $x \rightarrow \infty$ we note that the integrand is real for all real t and thus that

$$\psi_{2n,0}^s = -\frac{2i}{\pi} \Re \left\{ \int_0^\infty \frac{\cosh [k\gamma(d-y)]}{\gamma \sinh k\gamma d} e^{ikxt} c_{2n}(t) dt \right\}. \quad (2.34)$$

It can now be shown by considering the integral around the contour formed by the quadrant $\Re\{t\} > 0$, $\Im\{t\} > 0$, with indentations around all the poles that

$$\psi_{2n,0}^s \sim \frac{i}{kd} \sum_{p=0}^{j_s} \epsilon_p t_p^{-1} \cos(p\pi y/d) \sin kxt_p c_{2n}(t_p) \quad \text{as } x \rightarrow \infty, \quad (2.35)$$

where $\epsilon_0 = 1$, $\epsilon_p = 2$ for $p \geq 1$.

We thus see that suitable multipoles for propagating modes, symmetric about both $y = 0$ and $x = 0$, are

$$\begin{aligned} \phi_{2n,0}^s(x, y) = H_{2n}(kr) \cos 2n\theta - \frac{2i}{\pi} \int_0^\infty \frac{e^{-k\gamma d}}{\gamma \sinh k\gamma d} \cosh k\gamma y \cos kxt c_{2n}(t) dt \\ + \frac{1}{kd} \sum_{p=0}^{j_s} \epsilon_p t_p^{-1} \cos(p\pi y/d) \cos kxt_p c_{2n}(t_p) \end{aligned} \quad (2.36)$$

$$\sim \frac{1}{kd} \sum_{p=0}^{j_s} \epsilon_p t_p^{-1} \cos(p\pi y/d) e^{\pm ikxt_p} c_{2n}(t_p) \quad \text{as } x \rightarrow \pm \infty. \quad (2.37)$$

Similarly

$$\begin{aligned} \phi_{2n+1,0}^s(x, y) &= H_{2n+1}(kr) \cos(2n+1)\theta - \frac{2i}{\pi} \int_0^\infty \frac{e^{-k\gamma d}}{\gamma \sinh k\gamma d} \cosh k\gamma y \sin kxt s_{2n+1}(t) dt \\ &\quad + \frac{1}{kd} \sum_{p=0}^{j_s} \epsilon_p t_p^{-1} \cos(p\pi y/d) \sin kxt_p s_{2n+1}(t_p) \quad (2.38) \end{aligned}$$

$$\sim \mp \frac{i}{kd} \sum_{p=0}^{j_s} \epsilon_p t_p^{-1} \cos(p\pi y/d) e^{\pm ikxt_p} s_{2n+1}(t_p) \quad \text{as } x \rightarrow \pm \infty. \quad (2.39)$$

For the modes antisymmetric about $y = 0$ we find

$$\begin{aligned} \phi_{2n,0}^a(x, y) &= H_{2n}(kr) \sin 2n\theta - \frac{2}{\pi} \int_0^\infty \frac{e^{-k\gamma d}}{\gamma \cosh k\gamma d} \sinh k\gamma y \sin kxt s_{2n}(t) dt \\ &\quad + \frac{2}{kd} \sum_{p=1}^{j_a} \tau_p^{-1} \sin((p-\frac{1}{2})\pi y/d) \sin kx\tau_p s_{2n}(\tau_p) \quad (2.40) \end{aligned}$$

$$\sim \mp \frac{2i}{kd} \sum_{p=1}^{j_a} \tau_p^{-1} \sin((p-\frac{1}{2})\pi y/d) e^{\pm ikx\tau_p} s_{2n}(\tau_p) \quad \text{as } x \rightarrow \pm \infty, \quad (2.41)$$

and

$$\begin{aligned} \phi_{2n+1,0}^a(x, y) &= H_{2n+1}(kr) \sin(2n+1)\theta - \frac{2}{\pi} \int_0^\infty \frac{e^{-k\gamma d}}{\gamma \cosh k\gamma d} \sinh k\gamma y \cos kxt c_{2n+1}(t) dt \\ &\quad + \frac{2}{kd} \sum_{p=1}^{j_a} \tau_p^{-1} \sin((p-\frac{1}{2})\pi y/d) \cos kx\tau_p c_{2n+1}(\tau_p) \quad (2.42) \end{aligned}$$

$$\sim \frac{2}{kd} \sum_{p=1}^{j_a} \tau_p^{-1} \sin((p-\frac{1}{2})\pi y/d) e^{\pm ikx\tau_p} c_{2n+1}(\tau_p) \quad \text{as } x \rightarrow \pm \infty, \quad (2.43)$$

where the integrands now have simple poles at $k\gamma d = \pm(p-\frac{1}{2})\pi i$, $p = 1, 2, \dots$, i.e. at $t = \pm\tau_p$ where

$$\tau_p = (1 - ((p-\frac{1}{2})\pi/kd)^2)^{\frac{1}{2}}, \quad p = 1, 2, \dots, j_a, \quad (2.44)$$

$$\tau_p = i(((p-\frac{1}{2})\pi/kd)^2 - 1)^{\frac{1}{2}}, \quad p \geq j_a + 1, \quad (2.45)$$

where

$$(j_a - \frac{1}{2})\pi < kd < (j_a + \frac{1}{2})\pi. \quad (2.46)$$

Note that if $kd < \frac{1}{2}\pi$, $j_a = 0$ and all the poles are imaginary. If this is the case $\phi_{n,0}^a(x, y)$ is exponentially small as $|x| \rightarrow \infty$.

Expansions for these multipoles in terms of polar coordinates can be obtained using the following identities (see, for example, Abramowitz & Stegun 1964, equations (9.1.42)–(9.1.45)).

$$\cosh k\gamma y \cos kxt = \sum_{q=0}^{\infty} \epsilon_q J_{2q}(kr) \cos 2q\theta c_{2q}(t), \quad (2.47)$$

$$\cosh k\gamma y \sin kxt = 2 \sum_{q=0}^{\infty} J_{2q+1}(kr) \cos(2q+1)\theta s_{2q+1}(t), \quad (2.48)$$

$$\sinh k\gamma y \cos kxt = -2i \sum_{q=0}^{\infty} J_{2q+1}(kr) \sin(2q+1)\theta c_{2q+1}(t), \quad (2.49)$$

$$\sinh k\gamma y \sin kxt = -2i \sum_{q=1}^{\infty} J_{2q}(kr) \sin 2q\theta s_{2q}(t). \quad (2.50)$$

The resulting expressions are

$$\phi_{n,0}^s(r, \theta) = H_n(kr) \cos n\theta + \sum_{q=0}^{\infty} E_s\{q, n; 0\} J_q(kr) \cos q\theta, \quad (2.51)$$

and

$$\phi_{n,0}^a(r, \theta) = H_n(kr) \sin n\theta + \sum_{q=1}^{\infty} E_a\{q, n; 0\} J_q(kr) \sin q\theta, \quad (2.52)$$

where

$$E_s\{2q, 2n; 0\} = -\frac{2i\epsilon_q}{\pi} \int_0^{\infty} \frac{e^{-k\gamma d} c_{2q}(t) c_{2n}(t)}{\gamma \sinh k\gamma d} dt + \frac{\epsilon_q}{kd} \sum_{p=0}^{j_s} \epsilon_p t_p^{-1} c_{2q}(t_p) c_{2n}(t_p), \quad (2.53)$$

$$E_s\{2q+1, 2n+1; 0\} = -\frac{4i}{\pi} \int_0^{\infty} \frac{e^{-k\gamma d} s_{2q+1}(t) s_{2n+1}(t)}{\gamma \sinh k\gamma d} dt + \frac{2}{kd} \sum_{p=0}^{j_s} \epsilon_p t_p^{-1} s_{2q+1}(t_p) s_{2n+1}(t_p), \quad (2.54)$$

$$E_a\{2q, 2n; 0\} = \frac{4i}{\pi} \int_0^{\infty} \frac{e^{-k\gamma d} s_{2q}(t) s_{2n}(t)}{\gamma \cosh k\gamma d} dt + \frac{4}{kd} \sum_{p=1}^{j_a} \tau_p^{-1} s_{2q}(\tau_p) s_{2n}(\tau_p) \quad (q > 0), \quad (2.55)$$

$$E_a\{2q+1, 2n+1; 0\} = \frac{4i}{\pi} \int_0^{\infty} \frac{e^{-k\gamma d} c_{2q+1}(t) c_{2n+1}(t)}{\gamma \cosh k\gamma d} dt + \frac{4}{kd} \sum_{p=1}^{j_a} \tau_p^{-1} c_{2q+1}(\tau_p) c_{2n+1}(\tau_p), \quad (2.56)$$

and

$$E_s\{2q, 2n+1; 0\} = E_s\{2q+1, 2n; 0\} = E_a\{2q, 2n+1; 0\} = E_a\{2q+1, 2n; 0\} = 0.$$

These expansions are all valid for $0 < r < 2d$, $-\pi < \theta < \pi$.

From (2.53)–(2.56) we have

$$\Re[E_s\{2q, 2n; 0\}] = -\delta_{qn} + \frac{\epsilon_q}{kd} \sum_{p=0}^{j_s} \epsilon_p t_p^{-1} c_{2q}(t_p) c_{2n}(t_p), \quad (2.57)$$

$$\Re[E_s\{2q+1, 2n+1; 0\}] = -\delta_{qn} + \frac{2}{kd} \sum_{p=0}^{j_s} \epsilon_p t_p^{-1} s_{2q+1}(t_p) s_{2n+1}(t_p), \quad (2.58)$$

$$\Re[E_a\{2q, 2n; 0\}] = -\delta_{qn} + \frac{4}{kd} \sum_{p=1}^{j_a} \tau_p^{-1} s_{2q}(\tau_p) s_{2n}(\tau_p) \quad (q > 0) \quad (2.59)$$

and

$$\Re[E_a\{2q+1, 2n+1; 0\}] = -\delta_{qn} + \frac{4}{kd} \sum_{p=1}^{j_a} \tau_p^{-1} c_{2q+1}(\tau_p) c_{2n+1}(\tau_p), \quad (2.60)$$

and thus we see that in all cases the term proportional to $J_n(kr)$ is cancelled out. The behaviour of these multipoles as kd approaches the various cut-off frequencies from above and below is discussed in the Appendix.

To calculate the imaginary parts of these multipoles we need to compute integrals of the form

$$\int_0^{\infty} \frac{f(t)}{g(t)} dt,$$

where $g(t) = 0$ at $t = x_0, \dots, x_j$, $x_0 > x_1 > \dots > x_j > 0$, $g'(x_p) \neq 0$ and $f(x_p) \neq 0$, $p = 0, \dots, j$. We note the fact that

$$\int_0^{2x} \frac{dt}{t-x} = 0$$

and thus

$$\int_0^\infty \frac{f(t)}{g(t)} dt = \int_{2x_0}^\infty \frac{f(t)}{g(t)} dt + \int_0^{2x_0} \left[\frac{f(t)}{g(t)} - \sum_{p=0}^j \frac{f(x_p)}{g'(x_p)(t-x_p)} \right] dt + \sum_{p=1}^j \int_{2x_p}^{2x_0} \frac{f(x_p)}{g'(x_p)(t-x_p)} dt. \quad (2.61)$$

All the singularities are in the second integral and the integrand is integrable on each side of each singularity. The third term can be evaluated explicitly; it is

$$\sum_{p=1}^j \frac{f(x_p)}{g'(x_p)} \ln \left(\frac{2x_0}{x_p} - 1 \right).$$

The case of the modified Bessel functions is much simpler as the integral representations that result do not contain singularities. The resulting expansions are

$$\phi_{n,m}^s(r, \theta) = K_n(k_m r) \cos n\theta + \sum_{q=0}^\infty E_s\{q, n; m\} I_q(k_m r) \cos q\theta, \quad (2.62)$$

and

$$\phi_{n,m}^a(r, \theta) = K_n(k_m r) \sin n\theta + \sum_{q=1}^\infty E_a\{q, n; m\} I_q(k_m r) \sin q\theta, \quad (2.63)$$

where

$$E_s\{2q, 2n; m\} = \epsilon_q \int_1^\infty \frac{e^{-k_m dt} c_{2q}(t) c_{2n}(t)}{\gamma \sinh k_m dt} dt, \quad (2.64)$$

$$E_s\{2q+1, 2n+1; m\} = 2 \int_1^\infty \frac{e^{-k_m dt} c_{2q+1}(t) c_{2n+1}(t)}{\gamma \sinh k_m dt} dt, \quad (2.65)$$

$$E_a\{2q, 2n; m\} = -2 \int_1^\infty \frac{e^{-k_m dt} s_{2q}(t) s_{2n}(t)}{\gamma \cosh k_m dt} dt \quad (q > 0), \quad (2.66)$$

$$E_a\{2q+1, 2n+1; m\} = -2 \int_1^\infty \frac{e^{-k_m dt} s_{2q+1}(t) s_{2n+1}(t)}{\gamma \cosh k_m dt} dt \quad (2.67)$$

and

$$E_s\{2q, 2n+1; m\} = E_s\{2q+1, 2n; m\} = E_a\{2q, 2n+1; m\} = E_a\{2q+1, 2n; m\} = 0,$$

in each case $m \geq 1$.

Alternatively, for these multipoles we can write the integrals in terms of the original variable $v = \operatorname{arcosh} t$:

$$E_s\{2q, 2n; m\} = \epsilon_q (-1)^{n+q} \int_0^\infty \frac{e^{-k_m d \cosh v}}{\sinh(k_m d \cosh v)} \cosh 2qv \cosh 2nv dv, \quad (2.68)$$

$$E_s\{2q+1, 2n+1; m\} = -2(-1)^{n+q} \int_0^\infty \frac{e^{-k_m d \cosh v}}{\sinh(k_m d \cosh v)} \sinh(2q+1)v \sinh(2n+1)v dv, \quad (2.69)$$

$$E_a\{2q, 2n; m\} = 2(-1)^{n+q} \int_0^\infty \frac{e^{-k_m d \cosh v}}{\cosh(k_m d \cosh v)} \sinh 2qv \sinh 2nv dv \quad (q > 0), \quad (2.70)$$

$$E_n\{2q+1, 2n+1; m\} = -2(-1)^{n+q} \int_0^\infty \frac{e^{-k_m d \cosh v}}{\cosh(k_m d \cosh v)} \cosh(2q+1)v \cosh(2n+1)v \, dv. \quad (2.71)$$

Again these expansions are valid for $0 < r < 2d$, $-\pi < \theta < \pi$.

3. The general radiation problem

In this section we will consider the general radiation problem for a vertical circular cylinder of radius $a < d$ placed symmetrically in the channel, occupying the region $r \leq a$, $-H \leq z \leq 0$ so that it extends throughout the fluid depth. We write

$$\phi(x, y, z) = Ua \sum_{m=0}^{\infty} f_m(z) \left(\sum_{n=0}^{\infty} \alpha_{n,m}^s \phi_{n,m}^s + \sum_{n=1}^{\infty} \alpha_{n,m}^a \phi_{n,m}^a \right). \quad (3.1)$$

The function $\phi(x, y, z)$ thus satisfies

$$\nabla^2 \phi = 0 \quad \text{in the fluid} \quad (3.2)$$

$$\text{and} \quad \partial \phi / \partial y = 0 \quad \text{on} \quad |y| = d. \quad (3.3)$$

Also ϕ behaves like a sum of outgoing plane waves as $|x| \rightarrow \infty$. On the body ($r = a$) we will assume the following general boundary condition

$$\frac{\partial \phi}{\partial r} = U \sum_{m=0}^{\infty} f_m(z) \left(\sum_{n=0}^{\infty} G_{n,m}^s \cos n\theta + \sum_{n=1}^{\infty} G_{n,m}^a \sin n\theta \right). \quad (3.4)$$

Now if we define

$$\mathcal{H}_{q,m}(r) = \begin{cases} H_q(kr), & m = 0, \\ K_q(k_m r), & m \geq 1, \end{cases} \quad (3.5)$$

and

$$\mathcal{I}_{q,m}(r) = \begin{cases} J_q(kr), & m = 0, \\ I_q(k_m r), & m \geq 1, \end{cases} \quad (3.6)$$

$$\text{then} \quad \phi_{n,m}^s(r, \theta) = \sum_{q=0}^{\infty} [\mathcal{H}_{q,m}(r) \delta_{qn} + E_s\{q, n; m\} \mathcal{I}_{q,m}(r)] \cos q\theta, \quad (3.7)$$

$$\phi_{n,m}^a(r, \theta) = \sum_{q=1}^{\infty} [\mathcal{H}_{q,m}(r) \delta_{qn} + E_a\{q, n; m\} \mathcal{I}_{q,m}(r)] \sin q\theta, \quad (3.8)$$

and so

$$\begin{aligned} \phi = & Ua \sum_{q=0}^{\infty} \left\{ \sum_{m=0}^{\infty} f_m(z) \sum_{n=0}^{\infty} [\mathcal{H}_{q,m}(r) \delta_{qn} + E_s\{q, n; m\} \mathcal{I}_{q,m}(r)] \alpha_{n,m}^s \right\} \cos q\theta \\ & + Ua \sum_{q=1}^{\infty} \left\{ \sum_{m=0}^{\infty} f_m(z) \sum_{n=1}^{\infty} [\mathcal{H}_{q,m}(r) \delta_{qn} + E_a\{q, n; m\} \mathcal{I}_{q,m}(r)] \alpha_{n,m}^a \right\} \sin q\theta \end{aligned} \quad (3.9)$$

and

$$\begin{aligned} \left. \frac{\partial \phi}{\partial r} \right|_{r=a} = & Ua \sum_{q=0}^{\infty} \left\{ \sum_{m=0}^{\infty} f_m(z) \sum_{n=0}^{\infty} [\mathcal{H}'_{q,m}(a) \delta_{qn} + E_s\{q, n; m\} \mathcal{I}'_{q,m}(a)] \alpha_{n,m}^s \right\} \cos q\theta \\ & + Ua \sum_{q=1}^{\infty} \left\{ \sum_{m=0}^{\infty} f_m(z) \sum_{n=1}^{\infty} [\mathcal{H}'_{q,m}(a) \delta_{qn} + E_a\{q, n; m\} \mathcal{I}'_{q,m}(a)] \alpha_{n,m}^a \right\} \sin q\theta. \end{aligned} \quad (3.10)$$

If we also define

$$Z_{q,m} = \mathcal{J}'_{q,m}(a)/\mathcal{H}'_{q,m}(a), \quad (3.11)$$

which is complex if $m = 0$ but real otherwise, then the orthogonality of $f_n(z)$ over $(-H, 0)$ and of $\cos 2n\theta$, $\cos(2n+1)\theta$, $\sin 2n\theta$ and $\sin(2n+1)\theta$ over $(0, \pi)$ gives rise to the following systems of equations

$$\sum_{n=0}^{\infty} [\delta_{qn} + E_s\{2q, 2n; m\} Z_{2q,m}] \alpha_{2n,m}^s = \frac{G_{2q,m}^s}{a\mathcal{H}'_{2q,m}(a)}, \quad q \geq 0, \quad (3.12)$$

$$\sum_{n=0}^{\infty} [\delta_{qn} + E_s\{2q+1, 2n+1; m\} Z_{2q+1,m}] \alpha_{2n+1,m}^s = \frac{G_{2q+1,m}^s}{a\mathcal{H}'_{2q+1,m}(a)}, \quad q \geq 0, \quad (3.13)$$

$$\sum_{n=1}^{\infty} [\delta_{qn} + E_a\{2q, 2n; m\} Z_{2q,m}] \alpha_{2n,m}^a = \frac{G_{2q,m}^a}{a\mathcal{H}'_{2q,m}(a)}, \quad q \geq 1, \quad (3.14)$$

$$\sum_{n=0}^{\infty} [\delta_{qn} + E_a\{2q+1, 2n+1; m\} Z_{2q+1,m}] \alpha_{2n+1,m}^a = \frac{G_{2q+1,m}^a}{a\mathcal{H}'_{2q+1,m}(a)}, \quad q \geq 0 \quad (3.15)$$

($m \geq 0$ throughout). We note that if $G_{n,m}^s$ and $G_{n,m}^a$, $m \geq 1$ are real then all the terms in the equations with $m \geq 1$ are real and thus that all the coefficients $\alpha_{n,m}^s$ and $\alpha_{n,m}^a$ with $m \geq 1$ are real.

These expressions can then be substituted back into the expression for $\phi(r, \theta, z)$. We get

$$\begin{aligned} \phi(r, \theta, z) = & Ua \sum_{q=0}^{\infty} \left\{ \sum_{m=0}^{\infty} f_m(z) \left(\alpha_{q,m}^s \left[\mathcal{H}_{q,m}(r) - \frac{\mathcal{J}_{q,m}(r)}{\mathcal{J}'_{q,m}(a)} \mathcal{H}'_{q,m}(a) \right] + \frac{\mathcal{J}_{q,m}(r)}{a\mathcal{J}'_{q,m}(a)} G_{q,m}^s \right) \right\} \cos q\theta \\ & + Ua \sum_{q=1}^{\infty} \left\{ \sum_{m=0}^{\infty} f_m(z) \left(\alpha_{q,m}^a \left[\mathcal{H}_{q,m}(r) - \frac{\mathcal{J}_{q,m}(r)}{\mathcal{J}'_{q,m}(a)} \mathcal{H}'_{q,m}(a) \right] + \frac{\mathcal{J}_{q,m}(r)}{a\mathcal{J}'_{q,m}(a)} G_{q,m}^a \right) \right\} \sin q\theta. \end{aligned} \quad (3.16)$$

This expansion is valid for $r < 2d$. Now

$$J'_n(x)H_n(x) - H'_n(x)J_n(x) = -2i/\pi x$$

and

$$I'_n(x)K_n(x) - K'_n(x)I_n(x) = 1/x,$$

and so

$$(Ua)^{-1}\phi(a, \theta, z) =$$

$$\begin{aligned} & \sum_{q=0}^{\infty} \left\{ \frac{f_0(z)}{kaJ'_q(ka)} \left[J_q(ka)G_{q,0}^s - \frac{2i}{\pi} \alpha_{q,0}^s \right] + \sum_{m=1}^{\infty} \frac{f_m(z)}{k_m a I'_q(k_m a)} [\alpha_{q,m}^s + I_q(k_m a) G_{q,m}^s] \right\} \cos q\theta \\ & + \sum_{q=1}^{\infty} \left\{ \frac{f_0(z)}{kaJ'_q(ka)} \left[J_q(ka)G_{q,0}^a - \frac{2i}{\pi} \alpha_{q,0}^a \right] + \sum_{m=1}^{\infty} \frac{f_m(z)}{k_m a I'_q(k_m a)} [\alpha_{q,m}^a + I_q(k_m a) G_{q,m}^a] \right\} \sin q\theta. \end{aligned} \quad (3.17)$$

From (3.1) and the far-field behaviour of the multipoles we see that

$$\begin{aligned} (Ua)^{-1}\phi(x, y, z) \sim & \frac{f_0(z)}{kd} \left[\sum_{p=0}^{j_s} \frac{\epsilon_p}{t_p} \cos(p\pi y/d) e^{\pm ik_x t_p} \sum_{n=0}^{\infty} (\alpha_{2n,0}^s c_{2n}(t_p) \mp i\alpha_{2n+1,0}^s s_{2n+1}(t_p)) \right. \\ & \left. + \sum_{p=1}^{j_a} \frac{2}{\tau_p} \sin((p-\frac{1}{2})\pi y/d) e^{\pm ik_x \tau_p} \sum_{n=0}^{\infty} (\alpha_{2n+1,0}^a c_{2n+1}(\tau_p) \mp i\alpha_{2n,0}^a s_{2n}(\tau_p)) \right] \quad \text{as } x \rightarrow \pm \infty. \end{aligned} \quad (3.18)$$

This can be written

$$\phi(x, y, z) \sim -\frac{ig \cosh k(z+H)}{\omega \cosh kH} \left[\sum_{p=0}^{j_s} A_p^\pm \cos(p\pi y/d) e^{\pm ikxt_p} + \sum_{p=1}^{j_a} B_p^\pm \sin((p-\frac{1}{2})\pi y/d) e^{\pm ikxt_p} \right], \quad (3.19)$$

where
$$A_p^\pm = \frac{iUa \sinh kH \epsilon_p}{\omega d M_0^{\frac{1}{2}}} \sum_{n=0}^{\infty} (\alpha_{2n,0}^s c_{2n}(t_p) \mp i \alpha_{2n+1,0}^s s_{2n+1}(t_p)) \quad (3.20)$$

and
$$B_p^\pm = \frac{iUa \sinh kH}{\omega d M_0^{\frac{1}{2}}} \frac{2}{\tau_p} \sum_{n=0}^{\infty} (\alpha_{2n+1,0}^a c_{2n+1}(\tau_p) \mp i \alpha_{2n,0}^a s_{2n}(\tau_p)) \quad (3.21)$$

are the amplitudes of the various modes.

If we restrict our attention to rigid body motions then the normal velocity of a point on the body surface can be written

$$V(t) = \Re\{(U_1, U_2, U_3) + (U_4, U_5, U_6) \times \mathbf{r}\} \cdot \mathbf{n} e^{-i\omega t}, \quad (3.22)$$

where U_1, U_2, U_3 are the components of surge, sway and heave and U_4, U_5, U_6 are the components of roll, pitch and yaw. The vector $\mathbf{r} \equiv ((x-x_0), (y-y_0), (z-z_0))$ is the position vector of the point on the body surface with the origin at the centre of rotation, (x_0, y_0, z_0) , and $\mathbf{n} \equiv (n_1, n_2, n_3)$ is the unit outward normal. If we define $(n_4, n_5, n_6) = \mathbf{r} \times \mathbf{n}$ then the body boundary condition becomes

$$\frac{\partial \phi}{\partial n} = \sum_{i=1}^6 U_i n_i \quad (3.23)$$

and if ϕ is decomposed into six radiation potentials, one for each mode of motion, by

$$\phi = \sum_{i=1}^6 U_i \phi_i \quad (3.24)$$

then on the body we have

$$\partial \phi_i / \partial n = n_i, \quad i = 1, \dots, 6. \quad (3.25)$$

In the case of the vertical circular cylinder being considered here we have $\mathbf{n} = (\cos \theta, \sin \theta, 0)$, $\mathbf{r} \times \mathbf{n} = (z-z_0)(-\sin \theta, \cos \theta, 0)$ and thus heave and yaw can be ignored. We will also assume that the centre of rotation is $(0, 0, -\frac{1}{2}H)$.

The generalized hydrodynamic force on the body in the i th direction is given by

$$F_i(t) = \Re\{X_i e^{-i\omega t}\}, \quad i = 1, 2, 4, 5, \quad (3.26)$$

where
$$X_i = -i\rho\omega \int_{S_B} \phi n_i dS. \quad (3.27)$$

Here S_B is the body surface and for $i = 4, 5$ this is clearly a moment. We therefore have

$$X_i = -i\rho\omega \sum_{j=1, 2, 4, 5} U_j \int_{S_B} \phi_j n_i dS. \quad (3.28)$$

The force can be decomposed into a part in phase with the acceleration, the added mass coefficient, and a part in phase with the velocity, the damping coefficient. Thus we write

$$F_i = - \sum_{j=1, 2, 4, 5} (A_{ij} \ddot{\zeta}_j + B_{ij} \dot{\zeta}_j), \quad (3.29)$$

where

$$\zeta_j(t) = \Re\{\xi_j e^{-i\omega t}\} \quad (3.30)$$

is the displacement of the body surface in the j th mode. Thus

$$X_i = - \sum_{j=1, 2, 4, 5} U_j(-i\omega A_{ij} + B_{ij}) \quad (3.31)$$

and so

$$-i\omega A_{ij} + B_{ij} = i\rho\omega \int_{S_B} \phi_j n_i dS. \quad (3.32)$$

We will now concentrate on surge and sway motions as they will demonstrate all the qualitative features of results for problems of this type though it is possible to treat roll and pitch motions in a similar fashion.

For surge motion, which is symmetric about $y = 0$ and antisymmetric about $x = 0$, we write

$$\phi_1(x, y, z) = a \sum_{m=0}^{\infty} f_m(z) \sum_{n=0}^{\infty} \alpha_{2n+1, m}^s \phi_{2n+1, m}^s \quad (3.33)$$

and the body boundary condition is

$$\frac{\partial \phi_1}{\partial r} = \cos \theta = \cos \theta \sum_{m=0}^{\infty} f_m(z) G_{1, m}^s \quad \text{on } r = a, \quad (3.34)$$

where

$$G_{1, m}^s = F_m \equiv \frac{1}{H} \int_{-H}^0 f_m(z) dz = M_m^{-\frac{1}{2}} \frac{\sin k_m H}{k_m H}. \quad (3.35)$$

From (3.13) we see that the equations satisfied by the unknown coefficients are

$$\sum_{n=0}^{\infty} [\delta_{qn} + E_s \{2q+1, 2n+1; m\} Z_{2q+1, m}] \alpha_{2n+1, m}^s = \delta_{q0} F_m / a \mathcal{H}'_{1, m}(a), \quad (3.36)$$

where

$$q \geq 0, \quad m \geq 0,$$

which represents a set of infinite systems of equations, one for each value of m . To solve these systems numerically we must truncate them and so we solve for $q = 0, \dots, N$ and $m = 0, \dots, M$. In virtually all the problems that will be considered in this paper two truncation parameters, N and M , will be required. First, $N+1$ represents the number of multipoles used for each depth mode and, secondly, $M+1$ represents the number of depth modes used. Suitable values to take for N and M depend both on the problem and on what one is trying to compute. The values of N and M chosen varied with the problem being considered, but they are believed to give results accurate to within 1% in all cases.

We define non-dimensional added mass and damping coefficients for surge motion, μ_1 and ν_1 respectively, by

$$\mu_1 + i\nu_1 = (-i\omega A_{11} + B_{11})/i\omega M, \quad (3.37)$$

where $M \equiv \rho\pi a^2 H$ is the mass of fluid displaced by the cylinder. Thus from (3.17) and (3.32)

$$\mu_1 + i\nu_1 = \frac{F_0}{kaJ_1'(ka)} \left[J_1(ka)F_0 - \frac{2i}{\pi} \alpha_{1,0}^s \right] - \sum_{m=1}^{\infty} \frac{F_m}{k_m a I_1'(k_m a)} [\alpha_{1,m}^s + I_1(k_m a)F_m]. \quad (3.38)$$

Clearly the summation makes no contribution to the imaginary part of the right-hand side and so

$$\nu_1 = -\frac{2F_0}{\pi kaJ_1'(ka)} \Re\{\alpha_{1,0}^s\}. \quad (3.39)$$

This immediately shows that to compute the damping coefficient one only has to solve (3.36) with $m = 0$. A relation between the damping coefficient and the energy radiated down the channel can be found by applying Green's theorem to the functions ϕ_1 and $\phi_1 - \bar{\phi}_1$ (see, for example, Srokosz 1980). The resulting formula is

$$\nu_1 = \frac{4}{\pi kd} \sum_{p=0}^{j_s} \frac{\epsilon_p}{t_p} \left| \sum_{n=0}^{\infty} \alpha_{2n+1,0}^s \delta_{2n+1}(t_p) \right|^2 \quad (3.40)$$

and this was used as a check on all the results that have been computed.

Curves of μ_1 and ν_1 are shown for cylinders with a radius to depth ratio of 1/10 in figures 1 and 2. It was found that to achieve accurate values for the added mass coefficient it was necessary to use a fairly large number of depth modes and the figures show values computed using $M = 8$. However the number of multipoles required for each depth mode is small and a value of $N = 1$ was sufficient. Nine 2×2 systems of equations have thus been solved to compute each point on the curves. It was pointed out in II that for symmetric (about both $x = 0$ and $y = 0$) bodies in channels undergoing motions symmetric about $x = 0$ the hydrodynamic properties are characterized by spikes at or near the resonant frequencies of the channel and this can be attributed to the singular nature of $\phi_{2n,0}^s$ near the symmetric cut-off frequencies (see (A 3) and (A 4)). However, as is noted in the Appendix, $\phi_{2n+1,0}^s$ is not singular near the cut-off frequencies and so we do not expect the same spiky response for surge motion. We also expect any resonant response near $kd = n\pi$ to be greater for cylinders with smaller radius to channel semi-width ratios since large cylinders clearly inhibit the occurrence of transverse standing waves more than small ones. The figures confirm that in the case of surge there is very little resonant response near to the cut-off frequencies.

For sway motion, which is antisymmetric about $y = 0$ and symmetric about $x = 0$, we write

$$\phi_2(x, y, z) = a \sum_{m=0}^{\infty} f_m(z) \sum_{n=0}^{\infty} \alpha_{2n+1,m}^a \phi_{2n+1,m}^a \quad (3.41)$$

and the body boundary condition is

$$\frac{\partial \phi_2}{\partial r} = \sin \theta = \sin \theta \sum_{m=0}^{\infty} f_m(z) G_{1,m}^a \quad \text{on } r = a, \quad (3.42)$$

where

$$G_{1,m}^a = F_m. \quad (3.43)$$

From (3.15) we see that the equations satisfied by the unknown coefficients are

$$\sum_{n=0}^{\infty} [\delta_{qn} + E_a \{2q+1, 2n+1; m\} Z_{2q+1,m}] \alpha_{2n+1,m}^a = \frac{\delta_{q0} F_m}{a \mathcal{H}'_{1,m}(a)},$$

where

$$q \geq 0, \quad m \geq 0, \quad (3.44)$$

and we truncate this set of systems of equations as in the surge case above. We define non-dimensional added mass and damping coefficients for sway motion, μ_2 and ν_2 respectively, by

$$\mu_2 + i\nu_2 = (-i\omega A_{22} + B_{22})/i\omega M \quad (3.45)$$

and so from (3.17) and (3.32)

$$\mu_2 + i\nu_2 = \frac{F_0}{kaJ_1'(ka)} \left[J_1(ka)F_0 - \frac{2i}{\pi} \alpha_{1,0}^a \right] - \sum_{m=1}^{\infty} \frac{F_m}{k_m a I_1'(k_m a)} [\alpha_{1,m}^a + I_1(k_m a)F_m]. \quad (3.46)$$

Again the formula for the damping coefficient can be simplified, giving

$$\nu_2 = -\frac{2F_0}{\pi kaJ_1'(ka)} \Re\{\alpha_{1,0}^a\}. \quad (3.47)$$

The formula relating the damping coefficient to the radiated energy in this case is

$$\nu_2 = \frac{8}{\pi kd} \sum_{p=1}^{j_a} \frac{1}{\tau_p} \left| \sum_{n=0}^{\infty} \alpha_{2n+1,0}^a c_{2n+1}(\tau_p) \right|^2. \quad (3.48)$$

It was found that the convergence characteristics of the systems of equations (3.44) were very similar to the case of surge and so in all the following results values of $N = 1$ and $M = 8$ were used. Unlike the surge results, however, the results for sway contain many interesting features due to the singular nature of $\phi_{2n+1,0}^a$ near the antisymmetric cutoff frequencies (see (A 1) and (A 2)). Figures 3 and 4 show some typical results.

The curves show the added mass and damping coefficients for a cylinder for which $a/H = a/d = 0.1$. Figure 3 shows the added mass and we can see large spikes occurring just below the second and third cut-off frequencies, whereas just below the first cut-off frequency we can see the manifestation of a trapped mode frequency, a point at which the equations are singular. In this particular case the singular point occurs at a value of $kd/\pi \approx 0.4994$ ($kd \approx 1.569$) in agreement with the theory of Callan *et al.* (1991). (From the theory in their paper we note that the value kd at which the trapped mode occurs is independent of a/H .) Careful computation allows the sizes of the spikes to be determined and these are indicated in the figure. Figure 4 shows the damping coefficient which is zero for $kd < \frac{1}{2}\pi$ (as it must be since no waves are radiated down the channel and the damping coefficient is related to this energy through (3.48)) and which again exhibits extremely spiky behaviour. Note that the height of the spikes in the damping coefficient is almost exactly the same as the total height of the corresponding spikes in the added mass coefficient. This can be explained as follows. The damping and added mass coefficients are just the real and imaginary parts respectively of the complex force coefficient $q(\omega)$, say, for radiation problems, and spiky behaviour in these quantities corresponds to a pole in the lower half of the complex frequency plane close to the real axis. It can be shown that causality requires the force coefficient to be analytic in the upper half-plane (see, for example, Wehausen 1971). Near the pole ω_0 we have $q(\omega) = A(\omega - \omega_0)^{-1}$ approximately and as ω increases along the real ω axis a circle is described in the q plane. For the damping to be non-negative this circle, which passes through the origin, must have its centre on the positive real axis. As ω passes through the point nearest to ω_0 , $\Im q(\omega)$ passes through zero so that the peak of the damping spike coincides with a zero

of the added mass. It is also clear that the size of the damping spike and the total extent of the added-mass spike are both given by the diameter of the circle and are therefore equal. We are grateful to a referee for this explanation.

Results for a larger cylinder ($a/d = 0.3$) are shown in figures 5 and 6. Again we see the evidence of a trapped mode at $kd \approx 1.505$ and a spike just below the second antisymmetric cut-off frequency. However, in the case there is virtually no spike near the third antisymmetric cut-off. Again the height of the spike in the damping coefficient is very close to the total height of the spike in the added mass.

It should be noted that the height of the spikes is not monotonic as a/d increases, for example the peak in the damping coefficient just below the second antisymmetric cutoff frequency has heights of approximately 57.5, 12.7, and 20.1 for $a/d = 0.1, 0.2$ and 0.3 respectively.

4. The scattering problem

We will assume that there is an incident wave from $x = -\infty$ and so the problem is symmetric about $y = 0$. The problem can be written in the form of a radiation problem by writing the total potential Φ as

$$\Phi(x, y, z, t) = \Re\{\psi(x, y, z) e^{-i\omega t}\}, \quad (4.1)$$

where

$$\psi(x, y, z) = \phi(x, y, z) - \frac{igA \cosh k(z+H)}{\omega \cosh kH} e^{ikx}. \quad (4.2)$$

Here A represents the amplitude of the incident wave and we note that

$$\cosh k(z+H) = M_0^{\frac{1}{2}} f_0(z).$$

The function ϕ is a radiation potential which satisfies

$$\frac{\partial \phi}{\partial r} = \frac{igAM_0^{\frac{1}{2}}}{a\omega \cosh kH} f_0(z) \sum_{n=0}^{\infty} ka\epsilon_n i^n J'_n(ka) \cos n\theta \quad \text{on } r = a, \quad (4.3)$$

which is of the form of (3.4) with $U = -igAM_0^{\frac{1}{2}}/a\omega \cosh kH \equiv U_s$, say,

$$G_{2n,0}^s = -\epsilon_n (-1)^n ka J'_{2n}(ka), \quad (4.4)$$

$$G_{2n+1,0}^s = -2i(-1)^n ka J'_{2n+1}(ka) \quad (4.5)$$

and $G_{n,m}^s, G_{n,m}^a = 0$ otherwise. We thus write

$$\phi = U_s a f_0(z) \sum_{n=0}^{\infty} (\alpha_{2n,0}^s \phi_{2n,0}^s + \alpha_{2n+1,0}^s \phi_{2n+1,0}^s). \quad (4.6)$$

From (3.12) and (3.13) we see that the unknown coefficients satisfy

$$\sum_{n=0}^{\infty} [\delta_{qn} + E_s\{2q, 2n; 0\} Z_{2q,0}] \alpha_{2n,0}^s = -\epsilon_q (-1)^q Z_{2q,0}, \quad q \geq 0, \quad (4.7)$$

$$\sum_{n=0}^{\infty} [\delta_{qn} + E_s\{2q+1, 2n+1; 0\} Z_{2q+1,0}] \alpha_{2n+1,0}^s = -2i(-1)^q Z_{2q+1,0}, \quad q \geq 0. \quad (4.8)$$

Unlike the problems considered in the previous section we now have just two systems of equations to solve, each of which we truncate to an $(N+1) \times (N+1)$ system by letting q range from 0 to N . The systems converge extremely quickly and the results shown were all computed using a value of $N = 1$.

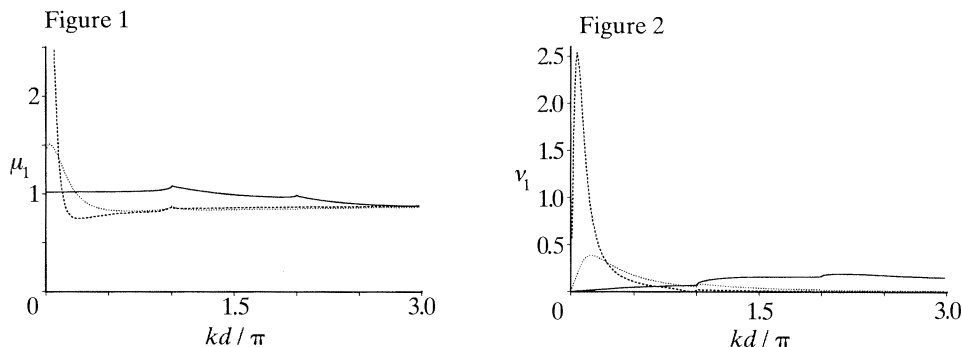


Figure 1. Surge added mass coefficient, μ_1 , plotted against kd/π for three cylinders with radius to channel semi-width ratios of 0.1 (—), 0.5 (····) and 0.9 (---). In all cases $a/H = 0.1$.

Figure 2. Surge-damping coefficient, ν_1 , plotted against kd/π for three cylinders with radius to channel semi-width ratios of 0.1 (—), 0.5 (····) and 0.9 (---). In all cases $a/H = 0.1$.

It follows from (3.18) that

$$\phi + U_s a f_0(z) e^{ikx} \sim U_s a f_0(z) \sum_{p=0}^{j_s} R_p \cos(p\pi y/d) e^{-ikxt_p} \quad \text{as } x \rightarrow -\infty, \quad (4.9)$$

$$\phi + U_s a f_0(z) e^{ikx} \sim U_s a f_0(z) \sum_{p=0}^{j_s} T_p \cos(p\pi y/d) e^{ikxt_p} \quad \text{as } x \rightarrow \infty, \quad (4.10)$$

where
$$R_p = \frac{\epsilon_p}{kdt_p} \sum_{n=0}^{\infty} [\alpha_{2n,0}^s c_{2n}(t_p) + i\alpha_{2n+1,0}^s s_{2n+1}(t_p)] \quad (4.11)$$

and
$$T_p = \delta_{0p} + \frac{\epsilon_p}{kdt_p} \sum_{n=0}^{\infty} [\alpha_{2n,0}^s c_{2n}(t_p) - i\alpha_{2n+1,0}^s s_{2n+1}(t_p)]. \quad (4.12)$$

In particular
$$R_0 = \frac{1}{kd} \sum_{n=0}^{\infty} (-1)^n [\alpha_{2n,0}^s + i\alpha_{2n+1,0}^s] \quad (4.13)$$

and
$$T_0 = 1 + \frac{1}{kd} \sum_{n=0}^{\infty} (-1)^n [\alpha_{2n,0}^s - i\alpha_{2n+1,0}^s]. \quad (4.14)$$

Applying Green's theorem to ψ and $\bar{\psi}$ leads to a result which represents the conservation of energy. It is

$$\sum_{p=0}^{j_s} \frac{t_p}{\epsilon_p} (|R_p|^2 + |T_p|^2) = 1 \quad (4.15)$$

and all results were checked against this formula.

It is straightforward to obtain from these formulas the behaviour of R_0 and T_0 in the limit as $kd \rightarrow 0$ with a/d fixed. We note that $Z_{0,0}$ and $Z_{1,0}$ are $O((kd)^2)$, whereas $Z_{n,0}$ is $O((kd)^4)$ for $n \geq 2$. A careful analysis of the size of the terms in (4.7) and (4.8) as $kd \rightarrow 0$ shows that

$$\alpha_{0,0}^s \sim -Z_{0,0} \sim -\frac{1}{4}\pi i(ka)^2, \quad (4.16)$$

$$\alpha_{1,0}^s \sim -2iZ_{1,0} \sim -\frac{1}{2}\pi(ka)^2, \quad (4.17)$$

whereas
$$\alpha_{n,0}^s = O((kd)^4). \quad (4.18)$$

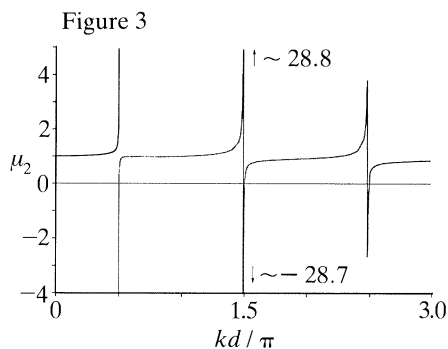


Figure 3. Sway added mass coefficient, μ_2 , plotted against kd/π for a cylinder with $a/d = 0.1$.

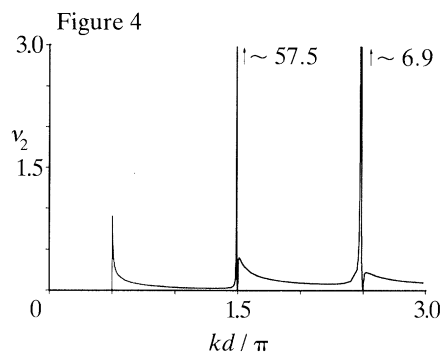


Figure 4. Sway damping coefficient, ν_2 , plotted against kd/π for a cylinder with $a/d = 0.1$.

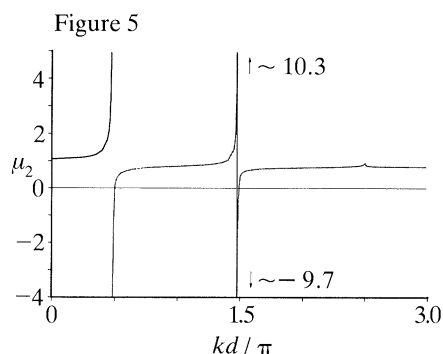


Figure 5. Sway added mass coefficient, μ_2 , plotted against kd/π for a cylinder with $a/d = 0.3$, $a/H = 0.1$.

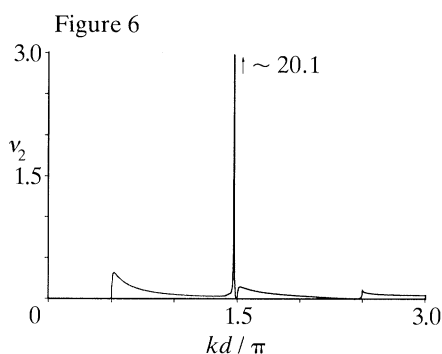


Figure 6. Sway damping coefficient, ν_2 , plotted against kd/π for a cylinder with $a/d = 0.3$, $a/H = 0.1$.

Thus from (4.13) and (4.14) we have

$$R_0 \sim -3\pi ika^2/4d \quad (4.19)$$

and

$$T_0 \sim 1 + \pi ika^2/4d \quad (4.20)$$

as $kd \rightarrow 0$, recovering a result obtained by a number of previous authors, a discussion of which can be found in Martin & Dalrymple (1988).

Typical results for the reflection and transmission coefficients for the various modes are shown in figures 7 and 8 which show plots for cylinders with $a/d = 0.5$ and 0.9 respectively. The curves show the energy associated with each reflected and transmitted mode (see (4.15) above) and thus at any particular value of kd/π the sum of the values of the curves is one.

The velocity potential on $r = a$ is given by (3.17) which simplifies to give

$$\phi(a, \theta, z) + U_s a f_0(z) e^{ika \cos \theta} = -\frac{2iU_s}{\pi k} f_0(z) \sum_{n=0}^{\infty} \frac{\alpha_{n,0}^s}{J'_n(ka)} \cos n\theta \quad (4.21)$$

and so the first-order force in the x direction is $\Re\{X e^{-i\omega t}\}$, where

$$X = \frac{1}{2} i Z_{1,0}^{-1} \alpha_{1,0}^s F \quad (4.22)$$

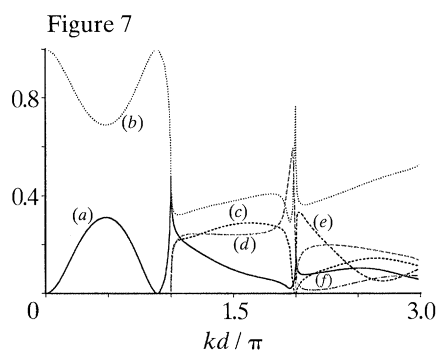


Figure 7. Energy associated with all the reflected and transmitted modes plotted against kd/π for a cylinder with $a/d = 0.5$. (a) $|R_0|^2$, (b) $|T_0|^2$, (c) $\frac{1}{2}t_1|R_1|^2$, (d) $\frac{1}{2}t_1|T_1|^2$, (e) $\frac{1}{2}t_2|R_2|^2$, (f) $\frac{1}{2}t_2|T_2|^2$.

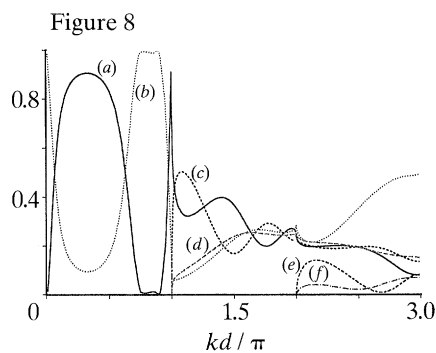


Figure 8. Energy associated with all the reflected and transmitted modes plotted against kd/π for a cylinder with $a/d = 0.9$. (a)–(f) as figure 7.

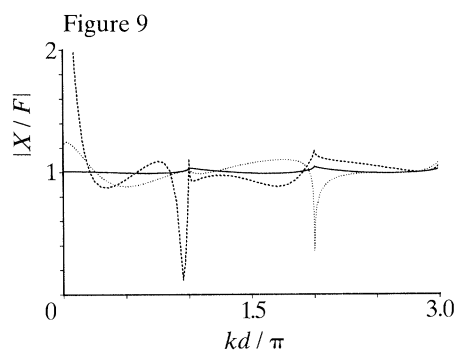


Figure 9. First-order force magnification factor, $|X/F|$, plotted against kd/π for three cylinders with radius to channel semi-width ratios of 0.1 (—), 0.5 (⋯) and 0.9 (---).

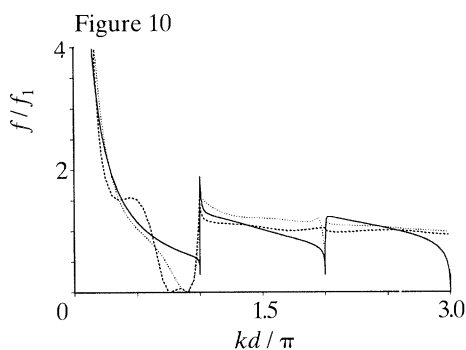


Figure 10. Mean second-order drift force magnification factor, f/f_1 , plotted against kd/π for three cylinders with radius to channel semi-width ratios of 0.1 (—), 0.5 (⋯) and 0.9 (---).

and

$$F = 4\rho g A \tanh(kH)/k^2 H'_1(ka)$$

is the force in the direction of wave advance on a single cylinder in the open sea (MacCamy & Fuchs 1954). A plot of $|X/F|$, which is clearly independent of a/H , for three different sized cylinder is shown in figure 9.

By using (4.21) the mean second-order drift force on the cylinder can be calculated as was done for a cylinder in an array of cylinders in Linton & Evans (1990). This results in

$$f = \frac{4\rho g A^2 H M_0}{\pi k a \sinh 2kH} \sum_{n=0}^{\infty} \epsilon_n^{-1} \left(\frac{n(n+1)}{(ka)^2} - 1 \right) \frac{\Re\{\alpha_{n,0}^s, \overline{\alpha_{n+1,0}^s}\}}{J'_n(ka) J'_{n+1}(ka)}. \quad (4.23)$$

This can be non-dimensionalized by the drift force on a vertical cylinder in the open sea which is given by

$$f_1 = \frac{16\rho g A^2 H M_0}{(\pi k a)^2 \sinh 2kH} \sum_{n=0}^{\infty} \left(\frac{n(n+1)}{(ka)^2} - 1 \right)^2 \frac{1}{|H'_n(ka)|^2 |H'_{n+1}(ka)|^2} \quad (4.24)$$

(see, for example, Linton & Evans 1990, equation (3.10)). Previous work on drift

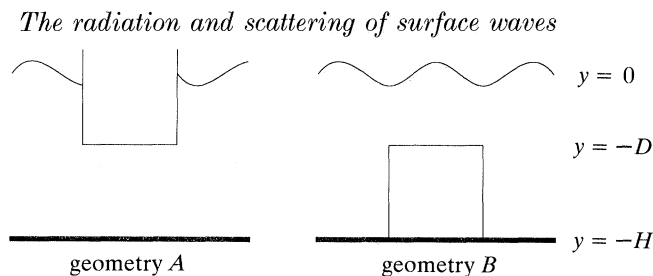


Figure 11. Definition sketch.

forces for bodies in channels is very limited. The reader is directed to Eatock Taylor & Hung (1985) for a more detailed discussion. A plot of f/f_1 for the same three cylinders as above is shown in figure 10.

5. Truncated cylinders

In this section we solve the radiation problems of surge, sway and heave together with the scattering problem for a truncated cylinder using channel multipoles. We consider two separate geometries here. Geometry *A* refers to a cylinder occupying the region $r \leq a$, $-D \leq z \leq 0$, whereas geometry *B* refers to a cylinder occupying the region $r \leq a$, $-H \leq z \leq -D$. The different geometries are illustrated in figure 11.

The procedure used is to construct inner and outer potentials and then match the velocity and pressure across the common boundary. We denote by L the interval $(-H, -D)$ in geometry *A* and $(-D, 0)$ in geometry *B* and by L^c the interval $(-H, 0) - L$.

The region $r > a$, $-H < z < 0$ is denoted by II and the velocity potential in this region, ϕ^{II} , is given by (3.9). In the inner region, region I, we need a different set of depth eigenfunctions and these are

$$g_m(z) = \begin{cases} e^{\frac{1}{2}\lambda_m z} \cos \lambda_m(z+D), & m \geq 0, \text{ geometry } A, \\ N_m^{-\frac{1}{2}} \cos \kappa_m(z+D), & m \geq 0, \text{ geometry } B, \end{cases} \quad (5.1)$$

where
$$\lambda_m = m\pi/(H-D), \quad (5.2)$$

$$N_m = \frac{1}{2} \left(1 + \frac{\sin 2\kappa_m D}{2\kappa_m D} \right), \quad (5.3)$$

and κ_m satisfies

$$\kappa_m \tan \kappa_m D + K = 0. \quad (5.4)$$

Here κ_m , $m \geq 1$, are real and positive, whereas $\kappa_0 = i\kappa$, κ real and positive. The functions $g_m(z)$ satisfy the orthogonality relations

$$\frac{1}{|L|} \int_L g_m(z) g_n(z) dz = \delta_{mn}, \quad (5.5)$$

where $|L|$ represents the length of the interval L . We also define

$$C_{mn} = \frac{1}{|L|} \int_L f_m(z) g_n(z) dz = \begin{cases} \left(\frac{\epsilon_n}{M_m} \right)^{\frac{1}{2}} \frac{k_m \sin k_m |L|}{|L|(k_m^2 - \lambda_n^2)} & \text{(geometry } A), \\ (M_m N_n)^{-\frac{1}{2}} \frac{k_m \sin k_m |L^c|}{|L|(k_m^2 - \kappa_n^2)} & \text{(geometry } B). \end{cases} \quad (5.6)$$

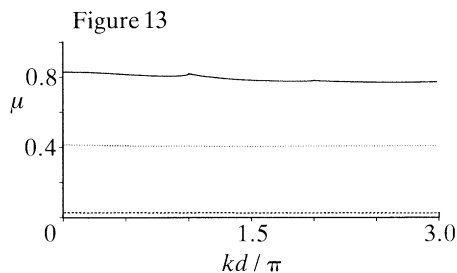
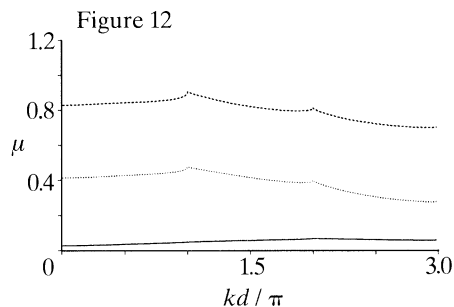


Figure 12. Surge added mass coefficient, μ , plotted against kd/π for three truncated cylinders, geometry *A*, with $D/H = 0.1$ (—), 0.5 (⋯) and 0.9 (---). In all cases $a/d = a/H = 0.1$.

Figure 13. Surge added mass coefficient, μ , plotted against kd/π for three truncated cylinders, geometry *B*, with $D/H = 0.1$ (—), 0.5 (⋯) and 0.9 (---). In all cases $a/d = a/H = 0.1$.

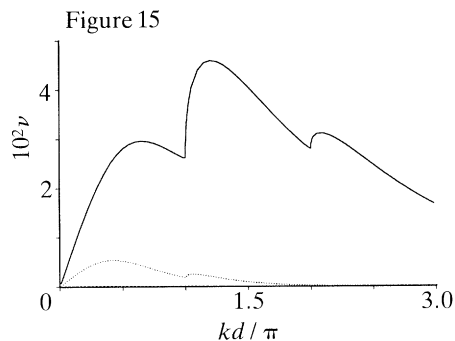
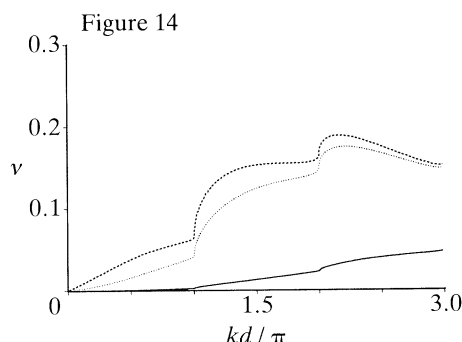


Figure 14. Surge damping coefficient, ν , plotted against kd/π for three truncated cylinders, geometry *A*, with $D/H = 0.1$ (—), 0.5 (⋯) and 0.9 (---). In all cases $a/d = a/H = 0.1$.

Figure 15. Surge damping coefficient, ν , plotted against kd/π for three truncated cylinders, geometry *B*, with $D/H = 0.1$ (—), 0.5 (⋯) and 0.9 (---). In all cases $a/d = a/H = 0.1$.

We start by considering geometry *A*. With the above depth eigenfunctions we can then write the inner potential as

$$\begin{aligned} \phi^I(r, \theta, z) = UP(r, z) + Ua \sum_{q=0}^{\infty} \left\{ \beta_{q,0}^s \left(\frac{r}{a} \right)^q + \sum_{m=1}^{\infty} \beta_{q,m}^s g_m(z) I_q(\lambda_m r) \right\} \cos q\theta \\ + Ua \sum_{q=1}^{\infty} \left\{ \beta_{q,0}^a \left(\frac{r}{a} \right)^q + \sum_{m=1}^{\infty} \beta_{q,m}^a g_m(z) I_q(\lambda_m r) \right\} \sin q\theta, \quad (5.7) \end{aligned}$$

where the harmonic function P is chosen so that ϕ^I satisfies the appropriate boundary condition on $z = -D$. Thus for surge and sway motions $P = 0$, whereas for heave motions we have

$$P(r, z) = \frac{1}{2}(H-D)^{-1} [\frac{1}{2}r^2 - (z+H)^2], \quad (5.8)$$

which ensures that

$$\partial \phi^I / \partial n = U \quad \text{on} \quad z = -D. \quad (5.9)$$

Note that for geometry *A* the unit normal out of the body on the bottom surface of the cylinder is $\mathbf{n} = (0, 0, -1)$. If we define

$$\mathcal{J}_{q,m}(r) = \begin{cases} (r/a)^q, & m = 0, \\ I_q(\lambda_m r), & m \geq 1, \end{cases} \quad (5.10)$$

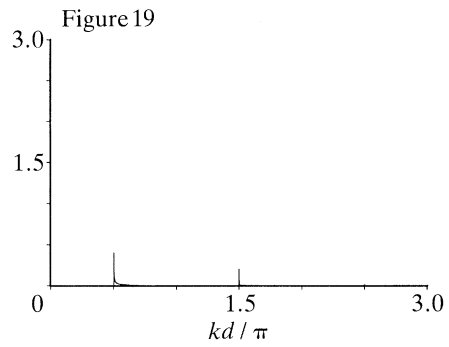
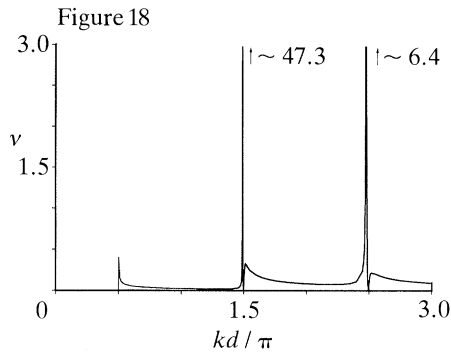
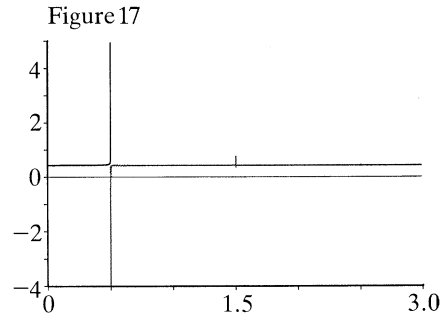
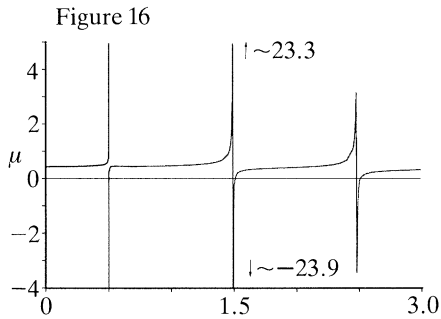


Figure 16. Sway added mass coefficient, μ , plotted against kd/π for a truncated cylinder, geometry *A*, with $a/d = a/H = 0.1$, $D/H = 0.5$.

Figure 17. Sway added mass coefficient, μ , plotted against kd/π for a truncated cylinder, geometry *B*, with $a/d = a/H = 0.1$, $D/H = 0.5$.

Figure 18. Sway damping coefficient, ν , plotted against kd/π for a truncated cylinder, geometry *A*, with $a/d = a/H = 0.1$, $D/H = 0.5$.

Figure 19. Sway damping coefficient, ν , plotted against kd/π for a truncated cylinder, geometry *B*, with $a/d = a/H = 0.1$, $D/H = 0.5$.

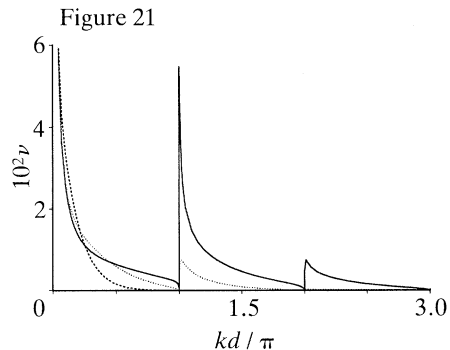
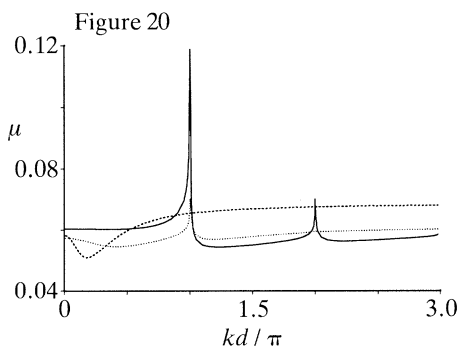


Figure 20. Heave added mass coefficient, μ , plotted against kd/π for three truncated cylinders, geometry *A*, with $a/d = 0.1$ (—), 0.2 (⋯) and 0.5 (---). In all cases $a/H = 0.1$, $D/H = 0.2$.

Figure 21. Heave damping coefficient, ν , plotted against kd/π for three truncated cylinders, geometry *A*, with $a/d = 0.1$ (—), 0.2 (⋯) and 0.5 (---). In all cases $a/H = 0.1$, $D/H = 0.2$.

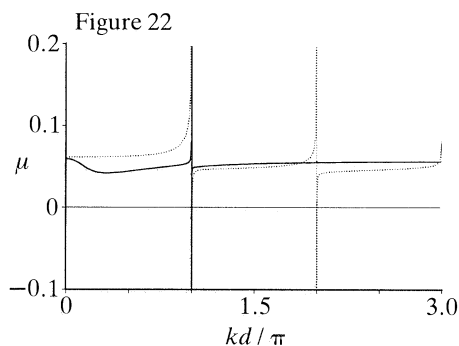


Figure 22. Heave added mass coefficient, μ , plotted against kd/π for two truncated cylinders, geometry B , with $a/d = 0.1$ (\cdots) and 0.4 (—). In both cases $a/H = 0.1$, $D/H = 0.2$.

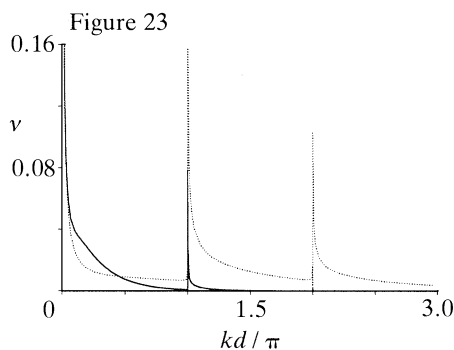


Figure 23. Heave damping coefficient, ν , plotted against kd/π for two truncated cylinders, geometry B , with $a/d = 0.1$ (\cdots) and 0.4 (—). In both cases $a/H = 0.1$, $D/H = 0.2$.

then

$$\phi^I(r, \theta, z) = UP(r, z) + Ua \sum_{m=0}^{\infty} g_m(z) \left\{ \sum_{q=0}^{\infty} \beta_{q,m}^s \mathcal{J}_{q,m}(r) \cos q\theta + \sum_{q=1}^{\infty} \beta_{q,m}^a \mathcal{J}_{q,m}(r) \sin q\theta \right\}. \quad (5.11)$$

If instead of defining $\mathcal{J}_{q,m}(r)$ by (5.10) we define it by

$$\mathcal{J}_{q,m}(r) = \begin{cases} J_q(\kappa r), & m = 0, \\ I_q(\kappa_m r), & m \geq 1, \end{cases} \quad (5.12)$$

and also choose

$$P(r, z) = z + K^{-1} \quad (5.13)$$

for heave motions, then (5.11) is a suitable form for geometry B as well. Thus both problems can now be solved simultaneously.

Continuity of the pressure across $r = a$ is equivalent to

$$\phi^I(a, \theta, z) = \phi^{II}(a, \theta, z) \quad z \in L. \quad (5.14)$$

The orthogonality of the trigonometric functions and application of the operator

$$\frac{1}{|L|} \int_L \dots g_n(z) dz$$

results in

$$\beta_{2q,n}^s \mathcal{J}_{2q,n}(a) = \sum_{m=0}^{\infty} C_{mn} \sum_{p=0}^{\infty} [\mathcal{H}_{2q,m}(a) \delta_{qp} + E_s\{2q, 2p; m\} \mathcal{J}_{2q,m}(a)] \alpha_{2p,m}^s - \frac{\delta_{q0}}{a|L|} \int_L P(a, z) g_n(z) dz, \quad (5.15)$$

$$\beta_{2q+1,n}^s \mathcal{J}_{2q+1,n}(a) = \sum_{m=0}^{\infty} C_{mn} \sum_{p=0}^{\infty} [\mathcal{H}_{2q+1,m}(a) \delta_{qp} + E_s\{2q+1, 2p+1; m\} \mathcal{J}_{2q+1,m}(a)] \alpha_{2p+1,m}^s, \quad (5.16)$$

$$\beta_{2q,n}^a \mathcal{J}_{2q,n}(a) = \sum_{m=0}^{\infty} C_{mn} \sum_{p=1}^{\infty} [\mathcal{H}_{2q,m}(a) \delta_{qp} + E_a\{2q, 2p; m\} \mathcal{J}_{2q,m}(a)] \alpha_{2p,m}^a \quad (q > 0), \quad (5.17)$$

$$\beta_{2q+1, n}^a \mathcal{J}_{2q+1, n}(a) = \sum_{m=0}^{\infty} C_{mn} \sum_{p=0}^{\infty} [\mathcal{H}_{2q+1, m}(a) \delta_{qp} + E_a\{2q+1, 2p+1; m\} \mathcal{J}_{2q+1, m}(a)] \alpha_{2p+1, m}^a, \quad (5.18)$$

for all $q, n \geq 0$.

Assuming continuity of the horizontal velocity on $r = a, z \in L$, and a general form for the boundary condition on $r = a, z \in L^c$ leads to the boundary condition

$$\frac{\partial \phi^{II}}{\partial r} = \begin{cases} \partial \phi^I / \partial r, & z \in L, \\ U \left(\sum_{n=0}^{\infty} G_n^s(z) \cos n\theta + \sum_{n=1}^{\infty} G_n^a(z) \sin n\theta \right), & z \in L^c. \end{cases} \quad (5.19)$$

The orthogonality of the trigonometric functions and application of the operator

$$\frac{1}{H} \int_{-H}^0 \dots f_n(z) dz$$

results in

$$\begin{aligned} \sum_{p=0}^{\infty} a[\mathcal{H}'_{2q, n}(a) \delta_{qp} + E_s\{2q, 2p; n\} \mathcal{J}'_{2q, n}(a)] \alpha_{2p, n}^s \\ = \frac{a|L|}{H} \sum_{m=0}^{\infty} C_{nm} \mathcal{J}'_{2q, m}(a) \beta_{2q, m}^s + \frac{\delta_{q0}}{H} \int_L \frac{\partial P}{\partial r}(a, z) f_n(z) dz + \mathcal{F}_{2q, n}^s, \end{aligned} \quad (5.20)$$

$$\begin{aligned} \sum_{p=0}^{\infty} a[\mathcal{H}'_{2q+1, n}(a) \delta_{qp} + E_s\{2q+1, 2p+1; n\} \mathcal{J}'_{2q+1, n}(a)] \alpha_{2p+1, n}^s \\ = \frac{a|L|}{H} \sum_{m=0}^{\infty} C_{nm} \mathcal{J}'_{2q+1, m}(a) \beta_{2q+1, m}^s + \mathcal{F}_{2q+1, n}^s, \end{aligned} \quad (5.21)$$

$$\begin{aligned} \sum_{p=1}^{\infty} a[\mathcal{H}'_{2q, n}(a) \delta_{qp} + E_a\{2q, 2p; n\} \mathcal{J}'_{2q, n}(a)] \alpha_{2p, n}^a \\ = \frac{a|L|}{H} \sum_{m=0}^{\infty} C_{nm} \mathcal{J}'_{2q, m}(a) \beta_{2q, m}^a + \mathcal{F}_{2q, n}^a \quad (q > 0), \end{aligned} \quad (5.22)$$

$$\begin{aligned} \sum_{p=0}^{\infty} a[\mathcal{H}'_{2q+1, n}(a) \delta_{qp} + E_a\{2q+1, 2p+1; n\} \mathcal{J}'_{2q+1, n}(a)] \alpha_{2p+1, n}^a \\ = \frac{a|L|}{H} \sum_{m=0}^{\infty} C_{nm} \mathcal{J}'_{2q+1, m}(a) \beta_{2q+1, m}^a + \mathcal{F}_{2q+1, n}^a \end{aligned} \quad (5.23)$$

for all $q, n \geq 0$, where

$$\mathcal{F}_{q, n}^s = \frac{1}{H} \int_{L^c} G_q^s(z) f_n(z) dz, \quad (5.24)$$

$$\mathcal{F}_{q, n}^a = \frac{1}{H} \int_{L^c} G_q^a(z) f_n(z) dz. \quad (5.25)$$

These equations can be combined with (5.15)–(5.18) to give a general set of infinite systems of equations. We get

$$\begin{aligned} & \sum_{p=0}^{\infty} a[\mathcal{H}'_{2q,n}(a) \delta_{qp} + E_s\{2q, 2p; n\} \mathcal{J}'_{2q,n}(a)] \alpha_{2p,n}^s \\ & \quad - \sum_{r=0}^{\infty} D_{nr,2q} \sum_{p=0}^{\infty} [\mathcal{H}_{2q,r}(a) \delta_{qp} + E_s\{2q, 2p; r\} \mathcal{J}_{2q,r}(a)] \alpha_{2p,r}^s \\ & = \frac{\delta_{q0}}{H} \int_L \left(\frac{\partial P}{\partial r}(a, z) f_n(z) - \sum_{m=0}^{\infty} C_{nm} \frac{\mathcal{J}'_{0,m}(a)}{\mathcal{J}_{0,m}(a)} P(a, z) g_m(z) \right) dz + \mathcal{F}_{2q,n}^s, \quad q, n \geq 0, \end{aligned} \quad (5.26)$$

$$\begin{aligned} & \sum_{p=0}^{\infty} a[\mathcal{H}'_{2q+1,n}(a) \delta_{qp} + E_s\{2q+1, 2p+1; n\} \mathcal{J}'_{2q+1,n}(a)] \alpha_{2p+1,n}^s \\ & \quad - \sum_{r=0}^{\infty} D_{nr,2q+1} \sum_{p=0}^{\infty} [\mathcal{H}_{2q+1,r}(a) \delta_{qp} + E_s\{2q+1, 2p+1; r\} \mathcal{J}_{2q+1,r}(a)] \alpha_{2p+1,r}^s \\ & = \mathcal{F}_{2q+1,n}^s, \quad q, n \geq 0, \end{aligned} \quad (5.27)$$

$$\begin{aligned} & \sum_{p=0}^{\infty} a[\mathcal{H}'_{2q,n}(a) \delta_{qp} + E_a\{2q, 2p; n\} \mathcal{J}'_{2q,n}(a)] \alpha_{2p,n}^a \\ & \quad - \sum_{r=0}^{\infty} D_{nr,2q} \sum_{p=0}^{\infty} [\mathcal{H}_{2q,r}(a) \delta_{qp} + E_a\{2q, 2p; r\} \mathcal{J}_{2q,r}(a)] \alpha_{2p,r}^a = \mathcal{F}_{2q,n}^a, \quad q \geq 1, \quad n \geq 0, \end{aligned} \quad (5.28)$$

$$\begin{aligned} & \sum_{p=0}^{\infty} a[\mathcal{H}'_{2q+1,n}(a) \delta_{qp} + E_a\{2q+1, 2p+1; n\} \mathcal{J}'_{2q+1,n}(a)] \alpha_{2p+1,n}^a \\ & \quad - \sum_{r=0}^{\infty} D_{nr,2q+1} \sum_{p=0}^{\infty} [\mathcal{H}_{2q+1,r}(a) \delta_{qp} + E_a\{2q+1, 2p+1; r\} \mathcal{J}_{2q+1,r}(a)] \alpha_{2p+1,r}^a \\ & = \mathcal{F}_{2q+1,n}^a, \quad q, n \geq 0, \end{aligned} \quad (5.29)$$

where

$$D_{nr,q} = \frac{a|L|}{H} \sum_{m=0}^{\infty} C_{nm} C_{rm} \frac{\mathcal{J}'_{q,m}(a)}{\mathcal{J}_{q,m}(a)}. \quad (5.30)$$

In the case of the cylinder extending throughout the depth we found that we obtained a different set of equations for each depth mode. We see from the equations above that for truncated cylinders this is no longer the case and all the depth modes are coupled.

For surge motion we write

$$\phi^I(r, \theta, z) = Ua \sum_{m=0}^{\infty} g_m(z) \sum_{q=0}^{\infty} \beta_{2q+1,m}^s \mathcal{J}_{2q+1,m}(r) \cos(2q+1)\theta, \quad (5.31)$$

$$\phi^{II}(r, \theta, z) = Ua \sum_{m=0}^{\infty} f_m(z) \sum_{q=0}^{\infty} \alpha_{2q+1,m}^s \phi_{2q+1,m}^s, \quad (5.32)$$

$G_1^s(z) = 1$ and $G_n^s(z) = G_n^a(z) = 0$ otherwise. The unknown coefficients $\alpha_{2q+1,m}^s$ and $\beta_{2q+1,m}^s$ can be found by solving (5.27) and then (5.16). If we truncate (5.27) by letting q range from 0 to N and n range from 0 to M we see that we have to solve an $(N+1)(M+1) \times (N+1)(M+1)$ system of equations. The added mass and damping

coefficients, non-dimensionalized in the same way as was done for the cylinder extending throughout the depth, are given by

$$\mu + i\nu = - \sum_{m=0}^{\infty} \mathcal{F}_{1,m}^s \left(\mathcal{H}_{1,m}(a) \alpha_{1,m}^s + \sum_{p=0}^{\infty} E_s\{1, 2p+1; m\} \mathcal{J}_{1,m}(a) \alpha_{2p+1,m}^s \right). \quad (5.33)$$

A check on the numerical results is provided by the relationship between the damping coefficient and the energy radiated down the channel which is given by (3.40). Values of $N = 1$ and $M = 8$ were again used to compute the results.

The effect of the length of a truncated cylinder on its hydrodynamic properties is illustrated by figures 12–15. Figures 12 and 13 show the added mass of cylinders with $D/H = 0.1, 0.5$ and 0.9 for both geometry *A* and geometry *B*. The curves show that the added mass depends on the length of the cylinder but that the values for a cylinder immersed through the free surface and for one resting on the bottom are very similar. As in the case of the cylinder extending throughout the depth there is very little resonant response near the cut-off frequencies with slightly more spiky behaviour in the case of geometry *A*.

In the case of the damping coefficient, shown in figures 14 and 15 we see that the different geometries produce markedly different results. This is not surprising since the damping coefficient is related to the wave making ability of a body and this is clearly going to be much greater in the case of a body which intersects the free surface than for one which is totally submerged.

For sway motion we write

$$\phi^I(r, \theta, z) = Ua \sum_{m=0}^{\infty} g_m(z) \sum_{q=0}^{\infty} \beta_{2q+1,m}^a \mathcal{J}_{2q+1,m}(r) \sin(2q+1)\theta, \quad (5.34)$$

$$\phi^{II}(r, \theta, z) = Ua \sum_{m=0}^{\infty} f_m(z) \sum_{q=0}^{\infty} \alpha_{2q+1,m}^a \phi_{2q+1,m}^a, \quad (5.35)$$

$G_1^a(z) = 1$ and $G_n^s(z) = G_n^a(z) = 0$ otherwise. The unknown coefficients $\alpha_{2q+1,m}^a$ and $\beta_{2q+1,m}^a$ can be found by solving (5.29) and then (5.18). The added mass and damping coefficients, non-dimensionalized as above, are given by

$$\mu + i\nu = - \sum_{m=0}^{\infty} \mathcal{F}_{1,m}^a \left(\mathcal{H}_{1,m}(a) \alpha_{1,m}^a + \sum_{p=0}^{\infty} E_a\{1, 2p+1; m\} \mathcal{J}_{1,m}(a) \alpha_{2p+1,m}^a \right). \quad (5.36)$$

The relation between the damping coefficient and the radiated energy is given by (3.48) in this case.

It was found that to achieve satisfactory convergence in the values for the added mass it was necessary to increase the number of multipoles used. Values of $N = 2$ and $M = 8$ were used in computing the results for added mass and damping shown in figures 16–19. Comparison with figures 3 and 4 shows that the results for a truncated cylinder immersed through the free surface are qualitatively the same as for the case of a cylinder extending throughout the depth. Away from the cut-off frequencies the value of the added mass for the truncated cylinder is less than that of the cylinder spanning the whole depth as was observed in the surge case above. The results for the case of a truncated cylinder on the bottom of the channel are rather different with the spikes near all but the first cut-off almost totally suppressed and again, as in the surface case, a very small damping coefficient. We note, however, that evidence for the existence of trapped modes appears in both cases.

Table 1. Values of kd at which trapped modes occur when $a/d = 0.5$, geometry A

D/H	a/H		
	0.05	0.1	0.5
0.05	1.48	1.54	1.57
0.1	1.41	1.47	1.57
0.2	1.39	1.41	1.55
0.5	1.39	1.39	1.48
0.9	1.39	1.39	1.41

Table 2. Values of kd at which trapped modes occur when $a/d = 0.5$, geometry B

D/H	a/H		
	0.05	0.1	0.5
0.05	1.55	1.49	1.32
0.1	1.57	1.55	1.40
0.2	1.57	1.57	1.47
0.5	1.57	1.57	1.55
0.9	1.57	1.57	1.57

Results for surge and sway with geometry A are given in III. Referring to figure 6a in their paper we see that they fail to predict the singular behaviour of the sway added mass coefficient below the first cut-off frequency.

With careful computation the values of kd at which the equations are singular can be computed for a variety of parameter values. Typical results are shown in tables 1 and 2 in which $a/d = 0.5$. From the theory of Callan *et al.* (1991) we know that the correct value for the trapped mode frequency for a cylinder spanning the whole depth with this radius to channel semi-width ratio is 1.391 to three decimal places. As was mentioned previously the value of kd at which the singularity occurs in this case is independent of a/H . In the case of truncated cylinders this is no longer the case.

Table 1 shows results accurate to two decimal places for geometry A for a range of values of a/H and D/H . We see that as $D/H \rightarrow 1$, corresponding to the gap below the cylinder tending to zero, the value of kd predicted for the trapped mode frequency appears to tend to the value predicted by Callan *et al.* (1991). Note that $\frac{1}{2}\pi \approx 1.571$ and a value of 1.57 in the table indicates a value of kd in the range $1.565 < kd < \frac{1}{2}\pi$. Table 2 shows the same set of results for geometry B . Now as the cylinder fills the entire water depth $D/H \rightarrow 0$ but we see that $kd \rightarrow 1.39$ in this limit. This is due to the fundamental difference between a problem where a body intersects the free surface and one where it does not. The singularity of the limit $D/H \rightarrow 0$ was noted by Miles (1983). We note also that for most parameter values in the table the value of kd at which a trapped mode occurs is very close to $\frac{1}{2}\pi$.

For heave motion we write

$$\phi^I(r, \theta, z) = UP(r, z) + Ua \sum_{m=0}^{\infty} g_m(z) \sum_{q=0}^{\infty} \beta_{2q, m}^s \mathcal{J}_{2q, m}(r) \cos 2q\theta, \quad (5.37)$$

$$\phi^{II}(r, \theta, z) = Ua \sum_{m=0}^{\infty} f_m(z) \sum_{q=0}^{\infty} \alpha_{2q, m}^s \phi_{2q, m}^s \quad (5.38)$$

and $G_n^s(z) = G_n^a(z) = 0$. The unknown coefficients $\alpha_{2q,m}^s$ and $\beta_{2q,m}^s$ can be found by solving (5.26) and then (5.15). The added mass and damping coefficients, non-dimensionalized as above, are given by

$$\mu + i\nu = \frac{2}{a^2 H} \left\{ \int_0^a rP(r, -D) dr + a \sum_{m=0}^{\infty} g_m(-D) \beta_{0,m}^s \int_0^a r\mathcal{J}_{0,m}(r) dr \right\}. \quad (5.39)$$

The final integral in this expression can always be evaluated explicitly since

$$\int_0^x tJ_0(t) dt = xJ_1(x)$$

(Abramowitz & Stegun 1964, equation 11.3.20), and

$$\int_0^x tI_0(t) dt = xI_1(x)$$

(Abramowitz & Stegun (1964), equation 11.3.25). Various integrals involving the function P are required and these are listed below. For geometry A we have

$$\int_0^a rP(r, -D) dr = \frac{1}{4}a^2 \left(\frac{a^2}{4|L|} - |L| \right), \quad (5.40)$$

$$\int_L P(a, z) g_0(z) dz = a|L| \left(\frac{a}{4|L|} - \frac{|L|}{6a} \right), \quad (5.41)$$

$$\int_L P(a, z) g_n(z) dz = -\frac{\sqrt{2}}{\lambda_n^2}, \quad n \geq 1, \quad (5.42)$$

$$\int_L \frac{\partial P}{\partial r}(a, z) f_n(z) dz = \frac{a \sin k_n |L|}{2k_n |L| M_n^{\frac{1}{2}}}, \quad n \geq 0, \quad (5.43)$$

whereas for geometry B we have

$$\int_0^a rP(r, -D) dr = \frac{1}{2}a^2(K^{-1} - D), \quad (5.44)$$

$$\int_L P(a, z) g_n(z) dz = -\frac{1}{N_n^{\frac{1}{2}} \kappa_n^2}, \quad n \geq 0, \quad (5.45)$$

$$\int_L \frac{\partial P}{\partial r}(a, z) f_n(z) dz = 0. \quad (5.46)$$

To achieve satisfactory convergence in the values for the added mass it was necessary to increase the number of depth modes and values of $N = 1$ and $M = 16$ were used to compute the results shown.

For geometry A this is the problem considered in I and II. Figures 20 and 21 show the added mass and damping coefficients for three cylinders with $a/H = 0.1$ and $D/H = 0.2$. The curves for $a/d = 0.1, 0.2$ and 0.5 correspond to those marked 10, 5 and 2 respectively in figure 5*a, b* in II. The different non-dimensionalization and scaling

account for the factor of 100. The curves for the damping coefficient show excellent agreement as do the added mass curves for $a/d = 0.1$ and 0.2 but the added mass curve for $a/d = 0.5$ is predicted to be slightly greater than the values shown in II.

Figures 22 and 23 show added mass and damping curves for a heaving truncated cylinder extending from the bottom, four fifths of the way to the free surface, again with $a/H = 0.1$. The figures show clearly how the larger cylinder suppresses the higher resonant frequencies.

To solve the scattering problem we write

$$\phi^I(r, \theta, z) = U_s a \sum_{m=0}^{\infty} g_m(z) \sum_{q=0}^{\infty} \beta_{q,m}^s \mathcal{J}_{q,m}(r) \cos q\theta, \quad (5.47)$$

$$\phi^{II}(r, \theta, z) = U_s a \left[f_0(z) \sum_{q=0}^{\infty} \epsilon_q i^q J_q(kr) \cos q\theta + \sum_{m=0}^{\infty} f_m(z) \sum_{q=0}^{\infty} \alpha_{q,m}^s \phi_{q,m}^s \right], \quad (5.48)$$

where $U_s = -igAM_0^3/a\omega \cosh kH$ as before. The application of the boundary conditions on $r = a$ results in the following two systems of equations:

$$\begin{aligned} & \sum_{p=0}^{\infty} a[\mathcal{H}'_{2q,n}(a) \delta_{qp} + E_s\{2q, 2p; n\} \mathcal{J}'_{2q,n}(a)] \alpha_{2p,n}^s \\ & - \sum_{r=0}^{\infty} D_{nr,2q} \sum_{p=0}^{\infty} [\mathcal{H}_{2q,r}(a) \delta_{qp} + E_s\{2q, 2p; r\} \mathcal{J}_{2q,r}(a)] \alpha_{2p,r}^s \\ & = \epsilon_q (-1)^q [D_{n0,2q} J_{2q}(ka) - \delta_{0n} ka J'_{2q}(ka)], \quad q, n \geq 0, \end{aligned} \quad (5.49)$$

and

$$\begin{aligned} & \sum_{p=0}^{\infty} a[\mathcal{H}'_{2q+1,n}(a) \delta_{qp} + E_s\{2q+1, 2p+1; n\} \mathcal{J}'_{2q+1,n}(a)] \alpha_{2p+1,n}^s \\ & - \sum_{r=0}^{\infty} D_{nr,2q+1} \sum_{p=0}^{\infty} [\mathcal{H}_{2q+1,r}(a) \delta_{qp} + E_s\{2q+1, 2p+1; r\} \mathcal{J}_{2q+1,r}(a)] \alpha_{2p+1,r}^s \\ & = 2i(-1)^q [D_{n0,2q+1} J_{2q+1}(ka) - \delta_{0n} ka J'_{2q+1}(ka)], \quad q, n \geq 0. \end{aligned} \quad (5.50)$$

Since the potential in region II is the same as for the scattering problem for a cylinder extending throughout the depth except for terms which decay exponentially as $|x| \rightarrow \infty$ the results concerning the far field, equations (4.9)–(4.15), all hold in this case also.

Results show that as kd increases the results for geometry *A* quickly tend to those for the case of a cylinder extending throughout the depth, as one would expect since very short waves are not influenced by the draught of the body. On the other hand in the case of geometry *B* short waves are not influenced by the presences of the body at all and results show that virtually all the energy is retained in the fundamental propagating mode ($|T_0|^2 \approx 1$) for all but the longest waves.

Figure 24 shows how the draught of a truncated cylinder immersed through the free surface for which $a/d = 0.9$ and $a/H = 0.1$ influences the value of the fundamental reflection coefficient. We can see that as the length of the cylinder is decreased the energy associated with the fundamental reflected mode is slightly decreased over the range $0 < kd < \frac{4}{5}\pi$, corresponding to $0 < ka < 2.26$, but that above this value the effect of the draught of the cylinder is negligible and the results are the same as those shown in figure 8.

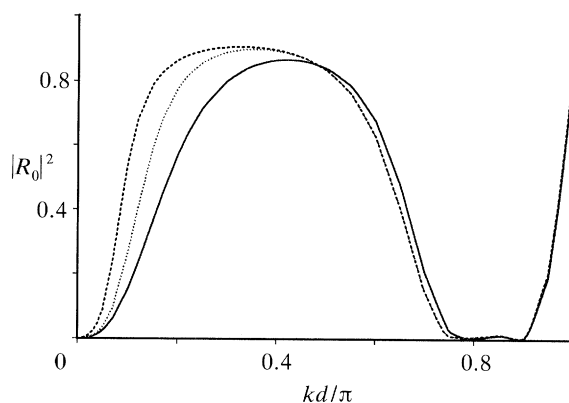
The radiation and scattering of surface waves

Figure 24. Energy associated with the fundamental reflected mode, $|R_0|^2$, for three truncated cylinders, geometry *A*, with $D/H = 0.1$ (—), 0.2 (⋯) and 0.5 (---). In all cases $a/H = 0.1$, $a/d = 0.9$.

6. Conclusion

In this paper we have developed new expressions for multipoles suitable for the solution of radiation and scattering problems concerning vertical circular cylinders situated on the centreline of a channel and either extending throughout the water depth or truncated so as to only fill part of the depth. The form of these multipoles shows very clearly the way the cut-off frequencies of the channel effect the far-field nature of the solution.

By using these multipoles we have solved a wide variety of different radiation and scattering problems and presented many results. Previous work on the hydrodynamic properties of bodies in channels has shown that the resonant frequencies of the channel can cause very ‘spiky’ behaviour. Here we have shown that, whereas this is the case for heave and sway motions, both of which are symmetric about a line perpendicular to the channel walls, it is not the case for surge motion which is antisymmetric about such a line. The different behaviour of the multipoles as kd approaches the resonant frequencies of the channel depending on their symmetry about a line across the channel explains why this is the case.

The method of solution is more powerful than previous methods used to solve similar problems. In particular the occurrence of modes other than the fundamental when $kd > \frac{1}{2}\pi$ is accurately modelled and the solutions are, in principle, exact. The problems considered in this paper have been formulated in a general way so that many different physical problems have been solved by essentially the same procedure.

All the problems considered have involved vertical circular cylinders situated on the centreline of a channel. The most obvious extension of the ideas in this paper would be the derivation of multipoles suitable for problems with cylinders placed at other points in the channel.

We thank Dr P. McIver for providing us with his notes on integral representations for wave functions and for many useful discussions. C.M.L. is supported by SERC under grant number GR/F/83969.

Appendix. Behaviour of channel multipoles near cut-off frequencies

We are interested in the behaviour of the $m = 0$ multipoles as kd approaches the cut-off frequencies for the channel. Specifically we wish to examine the limits

$$\lim_{kd \rightarrow j_s \pi^+} E_s\{q, n; 0\}, \quad \lim_{kd \rightarrow (j_s+1)\pi^-} E_s\{q, n; 0\}, \quad \lim_{kd \rightarrow (j_a-\frac{1}{2})\pi^+} E_a\{q, n; 0\}, \quad \lim_{kd \rightarrow (j_a+\frac{1}{2})\pi^-} E_a\{q, n; 0\}.$$

The particular case of $\lim_{kd \rightarrow \frac{1}{2}\pi^-} E_a\{2q+1, 2n+1; 0\}$ was considered in Callan *et al.* (1991) and only a brief description of the technicalities involved will be given here.

We will start by considering $E_a\{2q+1, 2n+1; 0\}$, defined by (2.56), in the limit as $kd \rightarrow (j_a + \frac{1}{2})\pi -$, $j_a = 0, 1, \dots$. Since τ_p^{-1} , $p = 1, \dots, j_a$ is bounded in this limit the real part of $E_a\{2q+1, 2n+1; 0\}$, given by (2.60) is bounded. If we split the imaginary part into two integrals, one from 0 to 1 and the other from 1 to infinity and then put $t = \sin u$ in the first of these, we can show that

$$\Im[E_a\{2q+1, 2n+1; 0\}] \sim -\frac{2}{\pi} \int_{-\frac{1}{2}\pi}^{\frac{1}{2}\pi} \tan(kd \cos u) \cos(2q+1)u \cos(2n+1)u \, du.$$

The value of the integral in the limit $kd \rightarrow (j_a + \frac{1}{2})\pi -$ can now be found by deforming the path of integration upwards over the pole at $u = i\chi$, where $kd \cosh \chi = (j_a + \frac{1}{2})\pi$. Thus we finally end up with the result that if $kd = (j_a + \frac{1}{2})\pi(1 - \frac{1}{2}\epsilon)$, $\epsilon > 0$, then

$$E_a\{2q+1, 2n+1; 0\} \sim -4i/(j_a + \frac{1}{2})\pi\epsilon^{\frac{1}{2}} \quad \text{as } \epsilon \rightarrow 0. \quad (\text{A } 1)$$

If we now consider the limit $kd \rightarrow (j_a - \frac{1}{2})\pi +$, $j_a = 1, 2, \dots$, we find that the imaginary part is bounded but now the real part is not and from (2.60) we see that if $kd = (j_a - \frac{1}{2})\pi(1 + \frac{1}{2}\epsilon)$, $\epsilon > 0$, then

$$E_a\{2q+1, 2n+1; 0\} \sim 4/(j_a - \frac{1}{2})\pi\epsilon^{\frac{1}{2}} \quad \text{as } \epsilon \rightarrow 0. \quad (\text{A } 2)$$

Next we consider $E_s\{2q, 2n; 0\}$, defined by (2.53). A similar analysis to the above shows that if $kd = (j_s + 1)\pi(1 - \frac{1}{2}\epsilon)$, $\epsilon > 0$, $j_s = 0, 1, \dots$, then

$$E_s\{2q, 2n; 0\} \sim -2\epsilon_q i/(j_s + 1)\pi\epsilon^{\frac{1}{2}} \quad \text{as } \epsilon \rightarrow 0, \quad (\text{A } 3)$$

whereas if $kd = j_s\pi(1 + \frac{1}{2}\epsilon)$, $\epsilon > 0$, $j_s = 1, 2, \dots$, then

$$E_s\{2q, 2n; 0\} \sim 2\epsilon_q/j_s\pi\epsilon^{\frac{1}{2}} \quad \text{as } \epsilon \rightarrow 0. \quad (\text{A } 4)$$

In deriving these results we have used the fact that $\lim_{t \rightarrow 0} c_n(t) = 1$. On the other hand $\lim_{t \rightarrow 0} s_n(t) = 0$ and we can use this to show that both $E_s\{2q+1, 2n+1; 0\}$ and $E_a\{2q, 2n; 0\}$ are bounded as kd approaches the cut-off frequencies from above or below.

References

- Abramowitz, M. & Stegun, I. A. 1964 *Handbook of mathematical functions*. New York: Dover.
- Çalışal, S. M. & Sabuncu, T. 1989 A study of a heaving vertical circular cylinder in a towing tank. *J. Ship Res.* **33** (2), 107–114.
- Callan, M., Linton, C. M. & Evans, D. V. 1991 Trapped modes in two-dimensional wave guides. *J. Fluid Mech.* **229**, 51–64.
- Eatock Taylor, R. & Hung, S. M. 1985 Mean drift forces on an articulated column oscillating in a wave tank. *Appl. Ocean Res.* **7** (2), 66–78.

- Erdélyi, A., Magnus, W., Oberhettinger, F. & Tricomi, F. G. 1953 *Higher transcendental functions*, vol. 2. McGraw-Hill.
- von Ignatowsky, W. 1914 Zur Theorie der Gitter. *Ann. Physik* **44**.
- von Ignatowsky, W. 1915 Über Reihen mit Zylinderfunctionen nach dem Vielfachen des Argumentes. *Archiv Mathematik Physik* **23**, 193–219.
- Lamb, H. 1945 *Hydrodynamics*. New York: Dover.
- Linton, C. M. & Evans D. V. 1990 The interaction of waves with arrays of vertical circular cylinders. *J. Fluid Mech.* **215**, 549–569.
- MacCamy, R. C. & Fuchs, R. A. 1954 Wave forces on piles: A diffraction theory. US Army Coastal Engineering Research Center, *Tech. Mem.* 69.
- Martin, P. A. & Dalrymple, R. A. 1988 Scattering of long waves by cylindrical obstacles and gratings using matched asymptotic expansions. *J. Fluid Mech.* **188**, 465–490.
- Miles, J. W. 1983 Surface-wave diffraction by a periodic row of submerged ducts. *J. Fluid Mech.* **128**, 155–180.
- Spring, B. H. & Monkmeyer, P. L. 1974 Interaction of plane waves with vertical cylinders. In *Proc. 14th Intl Conf. on Coastal Engineering*, ch. 107, pp. 1828–1848.
- Spring, B. H. & Monkmeyer, P. L. 1975 Interaction of plane waves with a row of cylinders. In *Proc. 3rd Conf. on Civil Eng in Oceans*, 979–998. Newark: ASCE.
- Srokosz, M. A. 1980 Some relations for bodies in a canal, with an application to wave-power absorption. *J. Fluid Mech.* **99**, 145–162.
- Thomas, G. P. 1991 The diffraction of water waves by a circular cylinder in a channel. *Ocean Engng* **18**, 17–44.
- Thorne, R. C. 1953 Multipole expansions in the theory of surface waves. *Proc. Camb. Phil. Soc.* **49**, 707–716.
- Twersky, V. 1952 Multiple scattering of radiation by an arbitrary configuration of parallel cylinders. *J. Acoust. Soc. Am.* **24**, 42–46.
- Twersky, V. 1956 On the scattering of waves by an infinite grating. *IRE Trans. Antennas Propagation* **4**, 330–345.
- Twersky, V. 1962 On scattering of waves by the infinite grating of circular cylinders. *IRE Trans. Antennas Propagation* **10**, 737–765.
- Wehausen, J. V. 1971 The motion of floating bodies. *A. Rev. Fluid Mech.* **3**, 237–268.
- Yeung, R. W. & Sphaier, S. H. 1989 Wave-interference effects on a truncated cylinder in a channel. *J. Engng Math.* **23**, 95–117.
- Yeung, R. W. & Sphaier, S. H. 1989 Wave-interference effects on a truncated cylinder in a towing tank. In *Proc. PRADS '89*. Varna, Bulgaria.
- Záviška, F. 1913 Über die Beugung elektromagnetischer Wellen an parallelen, unendlich langen Kreiszyklindern. *Ann. Physik* **40**, 1023–1056.

Received 24 April 1991; accepted 5 June 1991